Optimized Plasmonic On-Chip Refractive Index Sensor for Biosensing Applications

Authors:
Asma Rahman (190021128)
Samiha Ishrat (190021129)
Abdullah (190021132)

Supervisor:
Dr. Rakibul Hasan Sagor
Professor

A Thesis Submitted in Accordance with the Requirements of the Degree of

BACHELOR OF SCIENCE
IN
ELECTRICAL AND ELECTRONIC ENGINEERING

Islamic University of Technology
Board Bazar, Gazipur-1704, Bangladesh.

Department of Electrical and Electronic Engineering
June, 2024

Optimized Plasmonic On-Chip Refractive Index Sensor for Biosensing Applications

Approved by:

Dr. Rakibul Hasan Sagor

Supervisor and Professor,
Department of Electrical and Electronic Engineering,
Islamic University of Technology (IUT),
Boardbazar, Gazipur-1704.

Date: ……

Declaration of Authorship

This is to certify that the work presented in this thesis, titled **"Optimized Plasmonic On-Chip Refractive Index Sensor for Biosensing Applications"**, is the result of diligent research conducted under the guidance of **Dr. Rakibul Hasan Sagor, Professor, Department of Electrical and Electronic Engineering (EEE), Islamic University of Technology (IUT)**. This work was entirely completed during our candidacy for a Bachelor of Science (B.Sc.) degree at this university. There has been no prior submission of any part of this thesis for any other qualification or degree. All primary sources of assistance and the published work of others have been meticulously acknowledged in this thesis. In instances where a work has been quoted, the sources have been comprehensively cited.

____

Asma Rahman (190021128)

____

Samiha Ishrat (190021129)

____

Abdullah (190021132)

Acknowledgement

We are indebted to Allah (SWT), the Most Benevolent and Kind, for granting us the health, vigor, and capacity to research and compose this dissertation. His grace gave us the fortitude to endure all the obstacles that arose during our journey to this milestone. This work serves as a testament to the fact that aspirations can be transformed into accomplishments through perseverance, hard work, and faith.

We are deeply grateful to our supervisor, **Prof. Dr. Rakibul Hasan Sagor**, whose unwavering support has been a guiding beacon throughout this journey. The effectiveness of our thesis was significantly influenced by his mentorship, wisdom, and productive contributions. His profound comprehension of the subject matter, coupled with his unwavering faith in our abilities and immense patience, has significantly enhanced our academic experience and overall work ethic. We extend our sincere appreciation to him for his indispensable contribution.

We are also grateful to our family members for their unwavering support, love, prayers, and commitment to our lives. Their contributions have been instrumental in our progress toward achieving our objectives. Our achievements would not have been possible without their unwavering confidence in us, and their consistent encouragement has been instrumental in molding us into the individuals we are today.

This work would not have been feasible without the combination of all these efforts and influences. We express our heartfelt gratitude to all those who have contributed to our academic endeavor.

Table of Contents

List of Tables

List of Figures

List of Acronyms

CMOS	Complementary Metal Oxide Semiconductor
CO	Course Outcome
EM	Electro Magnetic
FEM	Finite Element Method
FOM	Figure of Merit
Hb	Hemoglobin
MIM	Metal-Insulator-Metal
MUS	Material Under Sensing
OBE	Outcome Based Education
PDE	Partial Differential Equation
PO	Program Outcome
RBC	Red Blood Cell
RI	Refractive Index
RIU	Refractive Index Unit
SERS	Surface-Enhanced Raman Scattering
SPP	Surface Plasmon Polariton
SPR	Surface Plasmon Resonance
TM	Transverse Magentic
TMD	Transition Metal Dichalcogenides
TMN	Transition Metal Nitrides
ZrN	Zirconium Nitride

Abstract

In-depth research into the design, fabrication, and utilization of plasmonic nanosensors is the focus of this study. This research is particularly emphasized on the unique capabilities of these sensors in detecting and analyzing molecular interactions at the nanoscale. A plasmonic refractive index nanosensor is a device that detects and quantifies changes in the refractive index of the ambient medium by utilizing the interaction of light with metallic nanoparticles. This allows for the detection of various analytes in a manner that is both extremely sensitive and label-free. These nanosensors generate an optical response that corresponds to the quantity being sensed through the use of surface plasmon polaritons (SPPs) and light-matter interaction. In this thesis, two designs for plasmonic refractive index sensors are proposed and assessed using the finite element method (FEM) with scattering boundary conditions, utilizing silver and ZrN materials. A meticulous explanation is provided of the theoretical foundations that underlie the functionalities and properties of plasmonic materials. Among the proposed designs, a plasmonic refractive index nanosensor with a modified rectangular resonator and a waveguide demonstrates a maximal sensitivity of 1650 nm/RIU. This sensor is exceptionally effective for a variety of applications due to its sensitivity, which is essential for detecting instant changes in the refractive index. To effectively identify unknown materials, the linear relationship between the refractive index and the resonant wavelength has been employed. The practical implementations of these nanosensor designs in the medical and healthcare sectors are reviewed, including the classification of cancer cells, detection of anemia and diabetes. Furthermore, the environmental and safety applications of these nanosensors are examined, with a particular emphasis on detecting heavy metals and chemical contaminants in water. This study provides a comprehensive examination of the diverse applications and fabrication processes of plasmonic nanosensors, illustrating their versatility and substantial influence in various fields. The sensitivity and overall performance of the proposed RI sensor are further improved by utilizing the distinctive properties of Zirconium Nitride (ZrN), a CMOS-compatible material renowned for its exceptional optical and electrical properties. Overall, the health, socio-cultural, economic, and ethical implications of plasmonic nanosensors have been extensively discussed. Furthermore, their applications in food safety and environmental sustainability underscore their ethical considerations and broader societal benefits.

Chapter 1

Introduction

Since there has been scientific research and technological advancement, humans have continuously endeavoured to unravel the mysteries of nature. People have always been interested in studying nature, events and the features of things or events. Humans have come up with many ways to measure things so that we can get a better idea of how big these things are. Numbers can be used to describe physical amounts and help us understand their sizes, shapes, and variations. Measuring things has become important in business, science, engineering, and engineering because it helps us understand the world around us better.

To study optics, a branch of science that looks at how light behaves and what its properties are, they need to be able to take precise measurements. To fully understand optical events, build optical systems, and make sure they work well, people need to be able to read things correctly. When it comes to optics, wavelength, strength, polarization, phase, and angle of a light wave are all very important. These steps must be taken in order to describe optical materials, check and set up optical gear, and study optical systems and their parts. For engineers and scientists to build new things and make lenses, mirrors, cameras, and lasers better, they need to know the right sizes. These tools are used in a lot of different fields, from photography and science to microscopy and making phone calls. When we test things and look at the data, it supports the ideas that led to them, so we learn more about optics.

Sensors are very important for measuring; they watch for changes in the world, write them down, and then use those changes as signs. Optical tools check for things like phase, polarity, range, light strength, and the refractive index. These tools accurately measure and explain light waves so that optical systems can be planned, set up, and made better. Some of the most important areas that use optical sensors are transmission, imaging, monitoring the sky, and microscopy. This is what they do because they know how to measure optical features properly.

This is a very new area of optical science that studies how electromagnetic fields change the electric charges in metals. Consistently spread out electron cycles happen where a metal and an insulator meet. These things happen because of how they work together. Plasmonics is a cutting-edge field that holds a lot of potential for making optical parts smaller and more complex in optical circuits and devices. Because it limits light to dimensions much smaller than its wavelength, plasmonics makes it possible for better camera systems and high-resolution sensors.

There are certain things about surface plasmons that make them great for many tasks, especially imaging and sensing. By changing surface plasmons, scientists can make imaging systems that don't let light bend too much and devices that are more sensitive than ever before. Sensors that use surface plasmon resonance (SPR) and surface plasmon polaritons (SPP) are very good at picking up on changes in the refractive index when they are close to a metal surface. We need this level of sensitivity for biosensing, which could use small changes in molecular make-up to find diseases early and keep an eye on biological processes.

Plasmonics has a huge amount of potential that goes far beyond the lab and touches many parts of everyday life. In medical diagnosis, plasmonic sensors are used to find biomarkers very accurately. This helps find diseases like diabetes, cancer, and infections early on. The components made of plasmonic matter could speed up the sending of data and make optical networks work better in the phone business. Plasmonic sensors can be used to keep an eye on the environment because they are so good at finding chemicals that change or are poisonous.
This study aims to improve plasmonic sensor technology so that it can be used in environmental monitoring, telecommunications, and medical diagnostics. This will help us understand and connect with our surroundings better.

1.1 Plasmonics

Plasmonics is a dynamic and swiftly advancing discipline that explores the identification, production, and control of optical signals at the nanoscale level. This interdisciplinary field integrates ideas from optics and nanotechnology, with a specific focus on the interactions between light and unbound electrons in metallic nanostructures. Plasmons are ensembles of oscillating electrons that exist at the interface between a metal and an uncharged substance. By illuminating them or providing them with external stimuli, we may observe and analyze them. An appropriate term to describe this phenomenon is "plasmonics." When this connection happens in certain places, electromagnetic fields are created. These fields can limit the size of light to dimensions much smaller than its wavelength. This enables the precise regulation of the interaction between light and matter [1].

Plasmonics is invaluable in numerous fields, including biosensing, due to its ability to obstruct light at a scale that is smaller than the wavelength. Because plasmon waves create strong electric fields, nanostructures are better at gathering and spreading light. They can fine-tune these nanostructures' plasmonic qualities by putting them together in the right way in terms of size, shape, and chemicals. Aside from that, this lets them change how the nanostructures pass light. Because matter and light can interact on purpose, it is possible to make sensors that are very delicate and can pick up on even the smallest changes in the refractive index [2]. This skill is necessary for biosensing purposes. The goal of our thesis project is to make a plasmonic on-chip refractive index monitor that is very good at sensing biological signals. Through the use of plasmonics concepts, our objective is to develop a sensor capable of executing several sensing operations on a single chip, exhibiting exceptional sensitivity and precision. Plasmonic nanostructures greatly increase the confinement and interaction of light, enabling our sensor to accurately detect changes in the refractive index. Because of this, it works well for keeping track of biological processes and figuring out what different proteins are.

Besides that, plasmonics lets us confine light beyond the diffraction limit, which is important for making optical parts smaller. This property is very useful for making small, effective photonic devices like light-emitting diodes, sensors, and waveguides. Our invention utilizes this potential to combine numerous sensing capabilities onto a single chip, hence improving the sensor's usefulness and adaptability. Two amazing visual effects that plasma plasmonic devices can show are surface-enhanced Raman scattering (SERS) and plasmon-enhanced fluorescence. Surface-enhanced Raman spectroscopy (SERS) can get molecules close to plasmonic nanoparticles to send out much stronger Raman scattering signals. This makes it easy and quick to find molecules. This method is very useful for scientists who study chemicals and living things because it helps them find very small amounts of molecules. Positron-enhanced fluorescence means that substances that glow can give off more light when they are near plasmonic structures. This makes fluorescence-based tests and imaging methods more sensitive. Our thesis project's main goal is to create a biosensor that is both very sensitive and flexible. This sensor's amazing reading abilities have a big impact on this goal. Because people are always looking for new ways to make things and new materials, the area of plasmonics is always changing. To make plasmonic elements, gold and silver are often used because they are so good at it. Currently, scientists are looking into different materials, such as graphene and transition metal dichalcogenides (TMDs), to improve the way machines work and do certain tasks. However, you can make nanostructures more plasmonic by carefully controlling their size, shape, and order. These days, it's easy to do because of tools like electron beam lithography and self-assembly. These tools allow researchers to precisely manipulate the properties of nanostructures for specific applications [3].

1.2 Surface Plasmon Polariton

Electromagnetic waves known as surface Plasmon Polaritons (SPPs) move along the interface between a conductor, usually a metal like gold or silver, and a dielectric (non-conducting) medium. The electromagnetic field's connection to the collective oscillations of free electrons at the metal-dielectric contact produces these waves. Because of their special qualities, SPPs are useful in many different domains, such as biosensing, optical communications, and nanophotonics. Rufus Ritchie first proposed the idea of surface plasmons in 1957. Research on SPPs has expanded dramatically over the years due to developments in technology and materials science, especially with the creation of tools like electron energy loss spectroscopy (EELS) and improvements in nanofabrication processes. These have made it possible to thoroughly investigate plasmonic phenomena at the nanoscale. SPPs are produced when electromagnetic waves interact with a metal's electron plasma. Surface-bound waves are formed at the interface between a metal and a dielectric due to the electromagnetic field's boundary conditions. With the right boundary conditions and Maxwell's equations, the dispersion relation for SPPs may be obtained. SPPs differ from other electromagnetic waves in a number of important ways, including the following qualities and traits:

Confinement and Localization: SPPs are very tightly bound to the interface between the metal and the dielectric, which makes it easier for electromagnetic energy to be focused at lengths much smaller than the wavelength of light in free space. Subwavelength confinement is a crucial characteristic that sets SPPs apart from traditional optical waves [4].

Dispersion: SPPs have a wave vector that is greater than light in open space, according to their dispersion relation. This results in increased momentum and slower phase velocity, which are essential for nanoscale light manipulation applications.

Propagation Length: The material characteristics and the operating wavelength determine the SPPs' propagation length, or the distance over which they retain their intensity. The use of metals with lower losses, such as gold and silver, is typically the key to achieving longer propagation lengths.

Improvement of the Field: SPPs can help surface-enhanced Raman scattering (SERS) applications that need strong interactions between light and matter because they can boost the electric field at the interface [5].

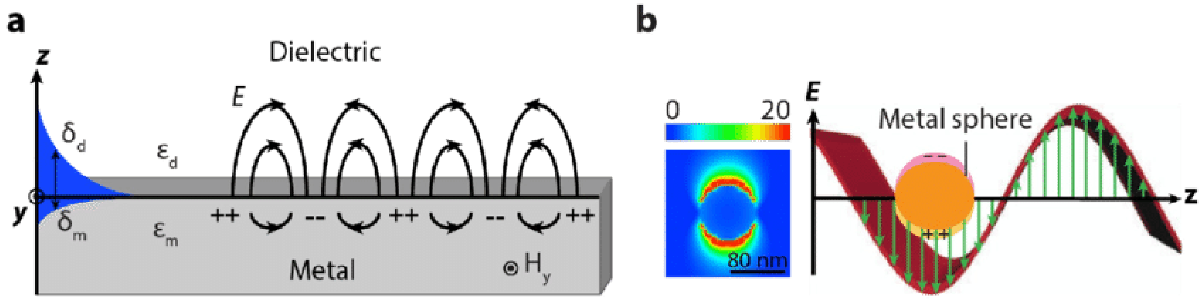

Figure 1.1: Propagation of SPP at Metal-Dielectric Interface

There are a variety of scientific and technological disciplines in which SPPs can be utilized in a variety of applications. The field of nanophotonics relies heavily on SPPs for the purpose of controlling light at the nanoscale. Plasmonic waveguides, couplers, and antennas are all examples of devices that make use of SPPs in order to produce photonic circuits that are both compact and efficient. As a result of their capacity to modify light in ways that are not attainable with conventional optics, these instruments are indispensable for the development of optical technologies that belong to the next generation. Due to the fact that SPPs are sensitive to changes in the dielectric environment, they are ideal for use in biosensing applications. Surface plasmon resonance (SPR) sensors are frequently used to identify biomolecular interactions in real time because of their high sensitivity and specificity combined with their ability to detect these interactions. Due to the fact that they are able to detect even the most minute variations in the refractive index at the boundary between the metal and the dielectric, these sensors are useful instruments for medical diagnostics. The enhancement of spectroscopy is another area in which SPPs have a significant impact. As a way to study molecules that are stuck to metal surfaces, surface-enhanced Raman scattering (SERS) and other methods use the field enhancement properties of SPPs to boost the Raman signal. This development makes it possible for spectroscopic analysis to achieve a level of sensitivity and precision that was previously unthinkable, enabling the ability to detect individual molecules. In addition to its applications in materials science, biology, and chemistry, SERS makes it possible to conduct in-depth molecular characterization.

Switches and modulators are examples of components that are necessary for integrated photonic circuits of the future. SPPs make it possible to develop ultra-compact, high-speed optical communication components, such as switches and modulators. The capability of these components to function at frequencies that are substantially higher than those of normal electrical systems makes it possible to process and transmit data at a faster rate. The growth of optical computing and telecommunications is contingent on the capability of incorporating these components into systems that are both tiny and efficient. The field of photovoltaics is yet another area in which SPPs are having a significant impact. Plasmonic structures might improve the efficiency of photovoltaic devices. This is because they can increase the amount of light that is trapped and improve where it is absorbed in solar cells. By utilizing the unique characteristics of SPPs, researchers will be able to develop solar cells that are capable of absorbing a greater amount of sunlight and converting it into electricity in a more efficient manner. This will contribute to the development of technology that utilizes renewable energy sources [7].

1.3 MIM Waveguide

A sophisticated kind of plasmonic waveguide known as a metal-insulator-metal (MIM) waveguide is composed of two metallic layers, usually noble metals like silver or gold, encased in a thin dielectric layer. Surface plasmon polaritons (SPPs) are electromagnetic waves that move along the edges of metal and dielectric. They permit light with much shorter wavelengths to be contained and guided compared to light in empty space. These structures are made to enable SPPs. Although the idea behind MIM waveguides dates back to plasmonics research in the early 20th century, the field saw substantial breakthroughs in the 1990s and early 2000s as a result of the advent of advanced nanofabrication methods like focused ion beam milling and electron-beam lithography. These methods made it possible to precisely construct the nanoscale structures required for MIM waveguides to function properly [8].

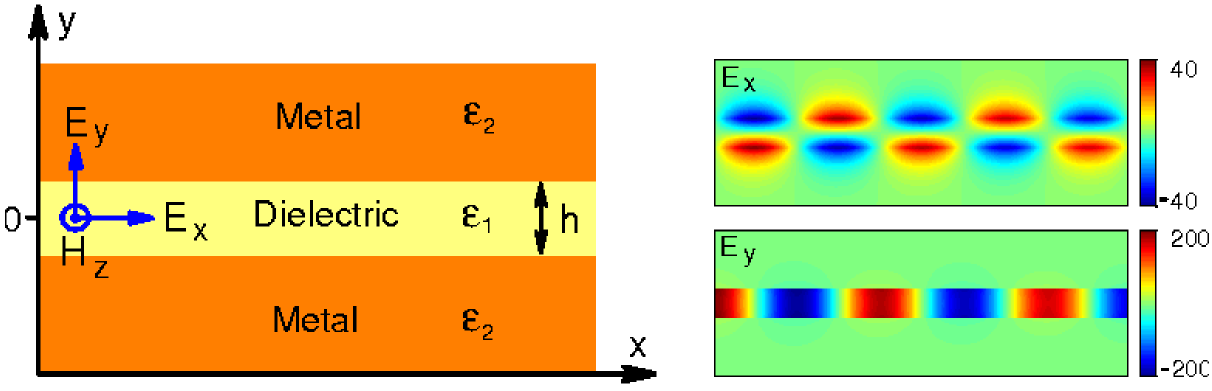

Figure 1.2: Configuration of MIM waveguide

Figure 1.2 demonstrates the configuration of MIM waveguide. The ability of MIM waveguides to create severe light confinement is one of their main features. This ability is important for the development of tiny photonic devices. Because the dielectric layer is so thin, the electromagnetic field is very concentrated at the metal-dielectric contacts in a MIM waveguide. This makes the field stronger and the modes more tightly bound. This characteristic is especially helpful for uses like nonlinear optics and sensors that require high-intensity electromagnetic fields at the nanoscale. Light is tightly packed in MIM waveguides, which makes it possible for very small photonic circuits and devices. This is possible because the effective wavelength of the guided modes is greatly reduced. Another essential component of MIM waveguides' operation is their dispersion characteristics. By varying the thickness of the dielectric layer and the material properties of the metals and the dielectric, it is possible to customize the dispersion relationship of SPPs in MIM systems. Depending on the needs of the application, this tunability allows the creation of waveguides with particular propagation characteristics, such as high confinement, low loss, or precise phase velocities [9]. Additionally, MIM waveguides support symmetric and antisymmetric modes, which are useful for a variety of photonic applications. Developing ultra-compact and extremely efficient photonic circuits is one of the most promising uses of MIM waveguides in the field of integrated photonics. These circuits have far smaller footprints than conventional optical components and are capable of performing a wide range of tasks, including switching, modulation, and signal processing.

MIM waveguides are also needed to make plasmonic sensors, which use SPPs' ability to respond to changes in the dielectric environment. Because these sensors are extremely sensitive to even the smallest changes in refractive index, they are perfect for environmental monitoring and biosensing applications. The increase in optical nonlinearities represents a substantial additional application domain for MIM waveguides. MIM structures offer considerable field enhancement and confinement, which can significantly boost the effectiveness of nonlinear optical processes like Kerr effects, four-wave mixing, and second-harmonic generation. This improvement is essential for creating efficient and small coherent light sources at novel wavelengths and for putting all-optical signal processing methods to use in photonic circuits. Moreover, efficient nano-antennas and metasurfaces—engineered surfaces with new capabilities to influence electromagnetic waves—can be made with MIM waveguides. With applications in imaging, sensing, and communication technologies, these structures can be made to accomplish certain tasks like focusing, beam steering, or polarization control. The development of on-chip light sources and detectors is also made possible by the ability to confine light to subwavelength dimensions in MIM waveguides. MIM waveguides, for instance, can be used with quantum dots or other nanoscale light-emitting substances to produce tiny, incredibly effective light sources. Similar to this, strong field augmentation can raise the interaction between directed light and active material, which in turn can enhance photodetectors' performance. MIM waveguides have many benefits, but they also have certain drawbacks, chief among them being losses. The propagation length of SPPs in MIM structures may be limited by the large absorption losses in the metal layers caused by the confinement of light to such small dimensions. Active plasmonic devices that incorporate gain materials to compensate for losses, hybrid plasmonic structures that combine MIM waveguides with dielectric waveguides, and the use of alternative materials with lower losses at optical frequencies are some of the strategies that have been suggested to mitigate these losses [10].

To sum up, metal-insulator-metal (MIM) waveguides are a useful and flexible tool in the field of nanophotonics because they offer high field enhancement, adjustable dispersion properties, and tight light confinement. Because of these characteristics, MIM waveguides are perfect for a variety of uses, such as plasmonic sensing, integrated photonics, nonlinear optics, and the creation of nano-antennas and metasurfaces. Even though losses are still a problem, ongoing research and development is enhancing the capabilities and performance of MIM waveguides to make the next generation of tiny photonic devices and systems possible.

1.4 RI Sensor

Refractive index (RI) sensors are highly developed optical instruments intended to quantify minuscule variations in a medium's refractive index. These variations might reveal diverse shifts in chemical composition, concentration, or the existence of particular compounds. The basis for these sensors' operation is the idea that changes in a medium's refractive index cause changes in the speed and direction of light passing through or reflecting off of it. Different configurations, including waveguides, interferometers, and surface plasmon resonance (SPR) sets, are used to measure this interaction. For example, surface plasmon polaritons (SPPs) are very sensitive to changes in the refractive index at the interface between the metal and dielectric. In SPR sensors, they are held up by a thin metal layer that is usually made of gold or silver. Any change in the sample's refractive index when it interacts with this contact changes the SPPs' resonance conditions, which can be measured and identified with great accuracy. Because RI sensors are sensitive to changes in refractive index, they can identify even the smallest alterations in a sample's composition. This makes them an invaluable tool in applications like biosensing, where they can precisely and sensitively track changes in biomolecular interactions in real time. Low analyte concentrations can be detected thanks to RI sensors, which can measure changes in refractive index at as low as 10^-6 RIU (refractive index units). RI sensors are used in environmental monitoring to find pollutants and other contaminants in soil, water, and the air. This provides vital information for determining regulatory compliance and environmental health. They are also used in industrial process control to ensure that tight manufacturing standards are followed by continuously monitoring the quality and consistency of products. The ability of RI sensors to be coupled with microfluidic systems, which permits the analysis of extremely small sample volumes and facilitates lab-on-a-chip applications, further increases their versatility. Because these integrated systems can quickly, with few sample requirements, complete sophisticated analyses, they are very helpful in the field of medical diagnostics [11].

The creation of nanoscale RI sensors, which offer even higher sensitivity and the capacity to detect single molecules, is a result of advancements in nanotechnology. The interaction between light and the analyte is better in these sensors because they use the unique properties of nanomaterials like quantum dots, carbon nanotubes, and nanoplasmonic structures. Because these tiny sensors can detect biomarkers at incredibly low concentrations, they hold great promise for personalized therapy and early illness diagnosis. Another significant type of RI sensor are optical fibre-based ones, in which variations in the surrounding medium's refractive index modify the fibre's capacity to transmit light. These sensors' flexibility, small size, and tolerance to electromagnetic interference make them ideal for dispersed and remote sensing applications.

Since they can provide real-time temperature, pressure, and chemical composition monitoring in demanding situations like oil and gas exploration, they are commonly employed in these settings. Additionally, in dynamic environments where circumstances change quickly and necessitate constant monitoring and quick feedback, the real-time operation of RI sensors offers substantial advantages. In applications like the manufacture of food and beverages, where real-time monitoring guarantees product safety and quality, this capability is essential. Additionally, RI sensors are employed in research and development to investigate basic chemical, biological, and physical phenomena. They can be used, for example, to track the development of biological tissues, look into the kinetics of chemical events, and examine how materials behave in various environmental settings. Field applications now have more options thanks to the development of portable and small-sized RI sensors, which enable on-location testing and analysis. In healthcare settings, where point-of-care diagnostics can yield rapid results and expedite medical action, this portability is especially advantageous. Although RI sensors provide many benefits, they also have drawbacks, including the demand for exact calibration, possible interference from external sources, and the need for specialized materials and fabrication methods. In order to overcome these obstacles, ongoing research and development is focused on strengthening sensor design, increasing sensitivity and selectivity, and creating reliable and affordable production procedures [12].

In conclusion, refractive index (RI) sensors are strong and adaptable instruments that use light's interaction with a medium to measure variations in the medium's refractive index with a high degree of specificity and sensitivity. They are used in many different domains, including industrial process control, biosensing, environmental monitoring, and medical diagnostics, where they offer vital data for process optimization and decision-making. Nanotechnology advancements and their integration with microfluidic systems are constantly expanding the capabilities and applications of RI sensors, which is encouraging for future developments that will have an even greater impact.

1.5 Motivation Behind The Study

A multimodal motivation behind our study aims to address numerous significant opportunities and demands in the field of integrated photonics and optical sensing. Using a single chip to accomplish simultaneous applications is one of the main objectives. Compact, multipurpose gadgets are in high demand in today's technology landscape. Conventional optical systems often require numerous discrete elements and components, which can be expensive, cumbersome, and difficult to combine. Our aim to create a multifunctional refractive index (RI) sensor on a single chip will enable us to drastically reduce the size, cost, and complexity of optical systems. This integration can streamline manufacturing and deployment processes while improving the sensor's performance and dependability. Such developments are crucial for applications where resources and space are limited, such as industrial process control, environmental monitoring, and biosensing [13].

One of the most significant benefits of integrating multiple applications on a single chip is the potential impact on human health diagnostics. For instance, a single-chip RI sensor could simultaneously monitor and diagnose conditions like anemia, cancer, and diabetes. Hemoglobin levels can aid in the detection of anemia, specific biomarkers can help detect cancer, and glucose levels can help monitor diabetes [4]. By combining these capabilities into one compact device, we can offer a powerful diagnostic tool that is more accessible and less invasive, improving patient outcomes and enabling more timely and accurate diagnoses.

Another strong incentive for our research is the investigation of alternative materials for RI sensor creation, specifically zirconium nitride (ZrN). Traditional materials like silicon and gold each have their benefits and drawbacks. Silicon is widely used due to its compatibility with existing semiconductor production processes, but its sensitivity and performance can be limited in certain wavelength ranges. Gold, on the other hand, offers excellent plasmonic properties but can be costly and challenging to integrate with other materials. By exploring ZrN, which has promising optical and electrical properties, we aim to achieve higher sensitivity, better performance, and lower costs. ZrN and other new materials like graphene and transition metal dichalcogenides (TMDs) could make RI sensors much more selective and sensitive, which would allow them to find lower concentrations of analyte and give more accurate results [7].

Furthermore, one of the primary goals of our research is to develop an RI sensor that is highly compatible with the complementary metal-oxide semiconductor (CMOS) industry. The CMOS sector underpins modern electronics, providing the manufacturing technique for integrated circuits used in almost all electronic devices. Creating RI sensors that can be seamlessly integrated into CMOS technology opens up numerous opportunities for mass production and deployment. By leveraging existing infrastructure and fabrication methods, CMOS-compatible sensors can reduce costs and shorten development cycles. This compatibility also facilitates the integration of optical sensors with electronic circuitry on the same chip, enabling advanced functionalities like real-time data processing, wireless connectivity, and on-chip signal conditioning. To achieve these objectives, our research focuses on innovative design strategies and production methods. We are looking into the use of hybrid plasmonic-dielectric structures, which have the benefits of both dielectric and plasmonic materials. For example, dielectric materials have low loss and are compatible with CMOS [9][10]. These hybrid structures can enhance light-matter interactions and improve the signal-to-noise ratio, thereby boosting the performance of RI sensors. Additionally, advanced nanofabrication techniques like electron-beam lithography and nanoimprinting allow for precise material patterning at the nanoscale, which is essential for creating highly sensitive and compact sensors.

In the realm of material investigation, we are examining the optical properties of innovative materials like graphene and TMDs, in addition to ZrN. Graphene is made up of a single layer of hexagonal carbon atoms arranged in a lattice. It has amazing electrical and optical properties, such as high carrier mobility and plasmonic resonances that can be tuned. These properties make graphene an attractive option for RI sensors, potentially offering greater sensitivity and faster response times than traditional materials. Similarly, TMDs—layered materials composed of transition metals and chalcogen atoms—possess unique optical qualities suitable for sensing applications. By incorporating these materials into our sensor designs, we aim to achieve superior performance and pioneer new approaches in optical sensing technologies. Creating CMOS-compatible RI sensors also demands careful consideration of material integration and fabrication techniques. CMOS technology relies on precise doping and etching processes on silicon-based substrates for integrated circuit manufacturing. Therefore, the materials and architecture we select for our RI sensors must align with these processes. This entails developing sensor structures that can be effortlessly integrated into the existing production workflow and selecting materials capable of withstanding the high temperatures and harsh chemical conditions associated with CMOS fabrication. By addressing these challenges, we aspire to create RI sensors that the semiconductor industry can readily adopt, facilitating their widespread use in various applications.

Ultimately, our research is motivated by the goal of advancing optical sensing through innovative architectures, new materials, and compatibility with existing systems. Investigating alternative materials for improved performance, achieving multiple tasks on a single chip, and ensuring CMOS technology compatibility represent significant strides towards developing next-generation RI sensors. These advancements promise to provide more precise, efficient, and cost-effective solutions for sensing and measurement applications in healthcare, environmental monitoring, industrial automation, and other fields. By integrating capabilities for anemia, cancer, and diabetes diagnosis onto a single chip, we can significantly enhance human health diagnostics. As we continue to push the boundaries of RI sensors, we remain committed to overcoming practical challenges and leveraging the latest scientific and technological developments to achieve our goals [14].

Chapter 2
Literature Review

Several designs and materials have been explored in the study of plasmonic refractive index (RI) sensors in an effort to improve performance and sensitivity. The main focus of these studies has been on using surface plasmon polaritons (SPPs) at the points where metals and dielectrics meet, making use of their ability to boost electromagnetic fields and resonate at certain frequencies. Strong electromagnetic confinement, quick detection speed, and ease of manufacture are features that set Metal-Insulator-Metal (MIM) waveguide-based sensors apart from other configurations [14-16].

As part of our effort, we resimulated a number of well-known designs from the literature to confirm their efficacy and sensitivity for various sensing applications. The potential of these sensors in real-world applications is shown by contrasting our resimulation results with those of the original studies. Surface Plasmon Polaritons (SPPs) are collective plasma oscillations that propagate at the metal-dielectric interface. These oscillations exhibit significant electromagnetic enhancement around nanoparticles and specific resonant frequencies, making them suitable for information transmission and sensing applications. SPP-based plasmonic nanosensors, particularly those utilizing Metal-Insulator-Metal (MIM) waveguides, are revolutionary due to their strong electromagnetic confinement, rapid and label-free detection capabilities, and ease of fabrication [15].

One such sensor explored is the high sensitivity plasmonic refractive index (RI) sensor designed for human blood group identification. The original study, "High Sensitivity Plasmonic Refractive Index Sensing and its Application for Human Blood Group Identification [2]" (Figure: 2.1(a)), utilized air and silver (Ag) materials. The transmission profiles demonstrated distinct peaks for refractive indices ranging from n=1 to n=1.1. In our resimulation, we observed similar transmission profiles with peaks at 1.2 µm, 1.3 µm, 1.4 µm, 1.5 µm, 1.6 µm, and 1.7 µm corresponding to n=1, n=1.02, n=1.04, n=1.06, n=1.08, and n=1.1, respectively. The sensitivity was calculated as 4500 nm/RIU. Another significant study, "Numerical Investigation of an Optimized Plasmonic On-Chip RI Sensor for Temperature and

Blood Group Detection [1]" (Figure: 2.1(b)), utilized materials such as MUS and Ag. This sensor was designed for temperature and blood group detection, with transmission spectra indicating responses to refractive indices of n=1, n=1.01, and n=1.02 in the wavelength range of 1000–2000 nm. In our resimulation, we observed transmission peaks at 1100 nm, 1200 nm, and 1300 nm for the corresponding refractive indices. The semi-circular MIM-based RI sensor for glucose detection, discussed in "Highly Sensitive MIM-Based Semi-Circular RI Sensor for Detection of Glucose Concentration [3]" (Figure: 2.1(c)), used MUS and Ag materials. The original transmission spectra for refractive indices n=1.525 to n=1.600 showed peaks between 2000-4000 nm. Our resimulation yielded similar results, with peaks shifting from 2100 nm to 2400 nm. The sensitivity calculated was 4000nm/RIU.

In "Plasmonic RI Sensing in the Early Diagnosis of Diabetes, Anemia, and Cancer: An Exploration of Biological Biomarkers [4]" (Figure: 2.1 (d)), dielectric, Ag, and air materials were used. The sensor's transmission profiles showed peak shifts for refractive indices n=1, n=1.01, and n=1.02. In our resimulation, we observed peaks at 1500 nm, 1600 nm, and 1700 nm, respectively. A highly sensitive triangular resonator-based plasmonic RI sensor was explored in "A Highly Sensitive Plasmonic Refractive Index Sensor Based on Triangular Resonator [5]" (Figure: 2.1(e)), utilizing air, dielectric, and silver materials. The original study showed peaks at 800-1300 nm for refractive indices n=1 to n=1.02. Our resimulation produced peaks at 850 nm, 900 nm, 950 nm, 1000 nm, and 1050 nm, demonstrating high sensitivity. The calculated sensitivity was 10000 nm/RIU.

The last paper, (Figure: 2.1(f)) "Plasmonic Refractive Index Sensor Based on Ring-Type Pentagonal Resonator with High Sensitivity [6]," used air, dielectric, and Ag. The sensor's transmission profiles for refractive indices n=1, n=1.01, and n=1.02 showed peaks in the 800-2200 nm range. In our resimulation, peaks were observed at 850 nm, 900 nm, and 950 nm, respectively. The sensitivity was calculated as follows:

$$\frac{950\,\mathrm{nm} - 850\,\mathrm{nm}}{1.02 - 1} = 5000\,\frac{\mathrm{nm}}{\mathrm{RIU}}.$$

Overall, our simulations showed that these plasmonic RI sensors are very sensitive and good at finding small changes in the refractive index. This is important for uses like identifying blood groups, keeping an eye on glucose levels, and finding diseases early on. The transmission profiles matched closely with the original studies, validating the sensors' designs and their potential for practical applications.

Here we provide a study of the original findings from multiple existing papers and the transmission characteristics from literature review. These findings demonstrate the practical applicability of these plasmonic RI sensors in various sensing applications. In order to improve the efficacy and effectiveness of lab-on-chip sensors, it is imperative to address this constraint and objectively improve the sensitivity of these sensors. For the purpose of developing a highly effective refractive index sensor that is suitable for a wide variety of applications, these literature reviews provided us with valuable insights into effective design and parameter settings.

(a)

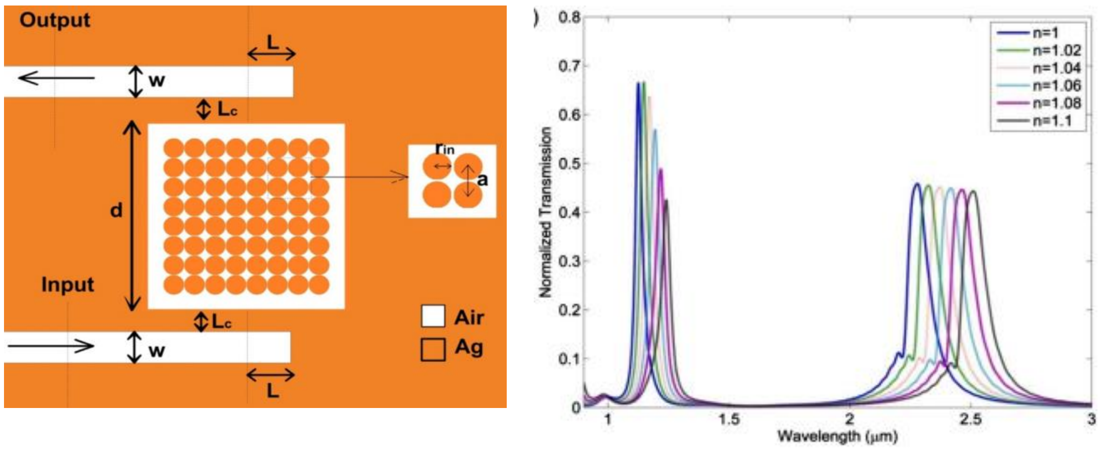

(b)

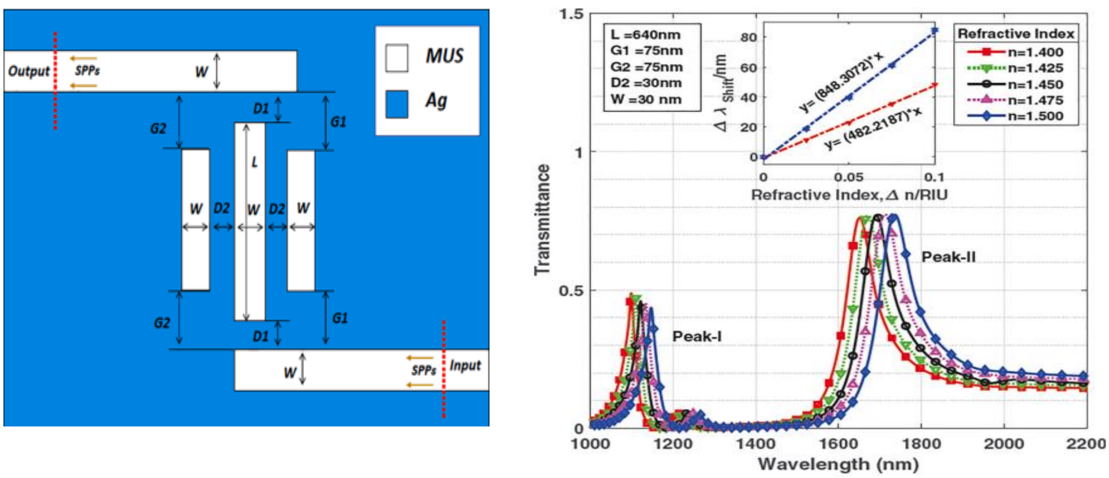

(c)

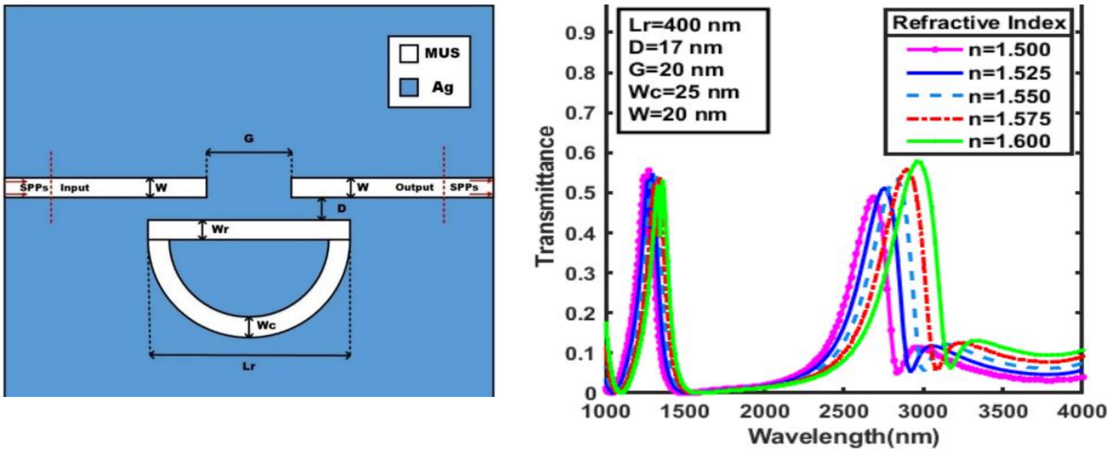
MUS
Ag
G
SPPs
Input
W
Output
D
Wr
Wc
Lr
Lr=400 nm
D=17 nm
G=20 nm
Wc=25 nm
W=20 nm
Refractive Index
n=1.500
n=1.525
n=1.550
n=1.575
n=1.600
Transmittance
Wavelength(nm)

(d)

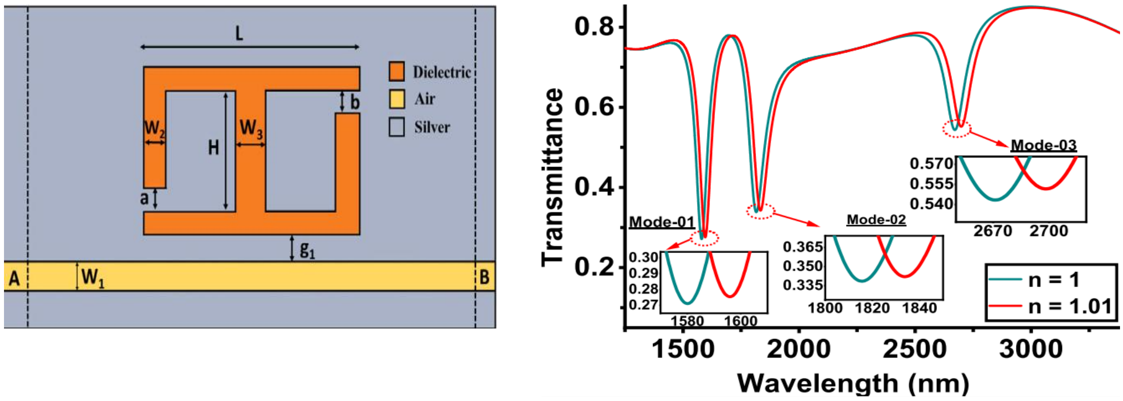
L
Dielectric
Air
Silver
b
H
a
g1
A
W1
B
Transmittance
Mode-01
Mode-02
Mode-03
n = 1
n = 1.01
Wavelength (nm)

(e)

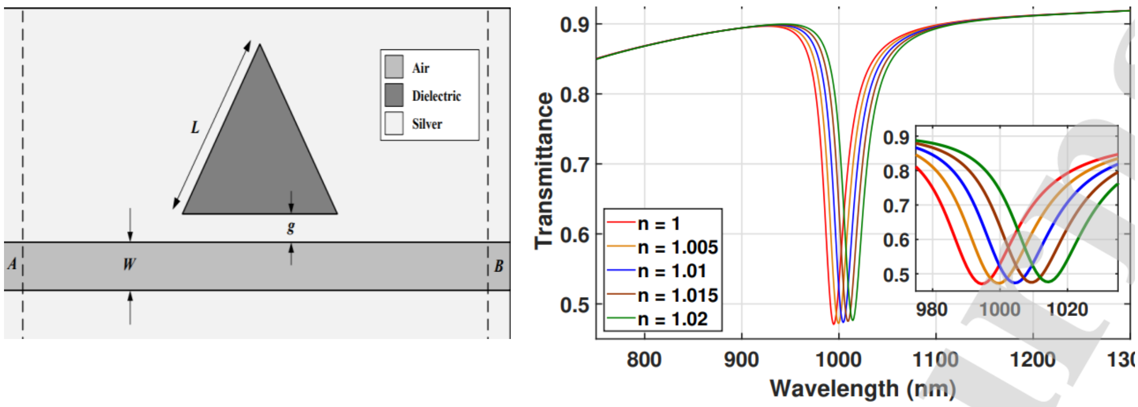
Air
Dielectric
Silver
L
g
W
A
B
Transmittance
n = 1
n = 1.005
n = 1.01
n = 1.015
n = 1.02
Wavelength (nm)

(f)

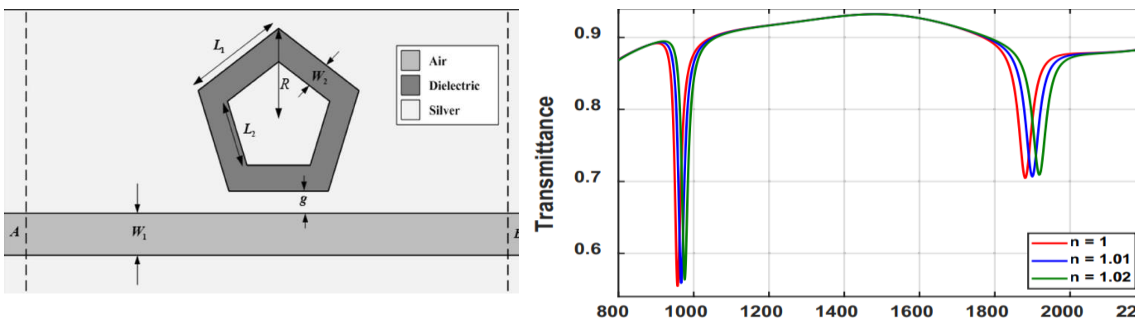
Air
Dielectric
Silver
R
g
Transmittance
n = 1
n = 1.01
n = 1.02

Figure 2.1: Different Transmission Characteristics from existing Literature reviews (a) High sensitivity plasmonic refractive index sensing and its application for human blood group identification [2] (b) Optimized plasmonic on-chip RI sensor for temperature and blood group detection [1] (c) Highly Sensitive MIM-Based Semi-circular RI Sensor for Detection of Glucose Concentration [3] (d) Plasmonic RI sensing in the early diagnosis of diabetes, anemia, and cancer [4] (e) Based on Triangular Resonator [5] (f) Based on Ring-Type Pentagonal Resonator with High Sensitivity [6].

A comparative analysis between the transmission characteristics that were obtained from our resimulations and the original findings that were collected from a number of different investigations is presented in the following table 2.1. This study was carried out in order to compare and contrast the two sets of data. This validation lends support to the theory that these plasmonic RI sensors can be utilized in a wide range of sensing applications from a practical standpoint.

On the other hand, when we have a look at the data that has been presented in Table 2.1, we can see that the sensitivity of these MIM-based refractive index (RI) sensors is not sufficient for optimal performance. This is something that we can see when we look at the data. In the process of looking at the data, we have come to the conclusion that this is the case. It is of the utmost importance to find a solution to this limitation and to take into account this objective in order to make lab-on-chip systems more efficient and effective. This will have the consequence of enabling these sensors to have a higher level of sensitivity.

Table 2.1: Comparison between Original figures and Resimulated results

	Original Simulation / Transmission Profile	**Resimulated Results**
(a)	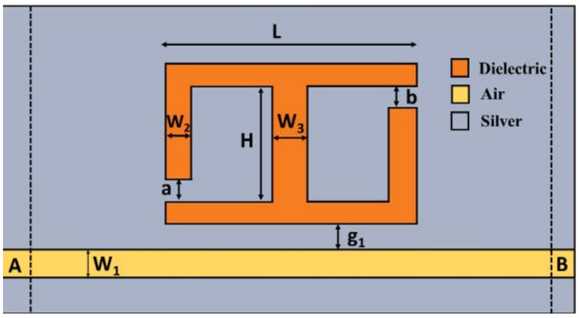	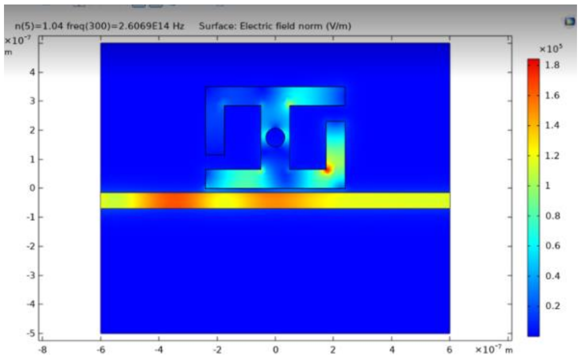
(b)	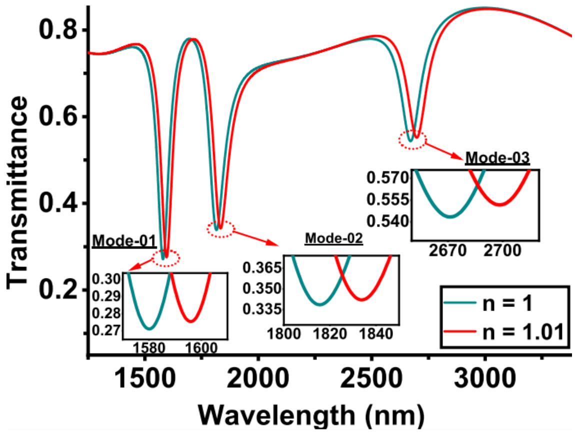	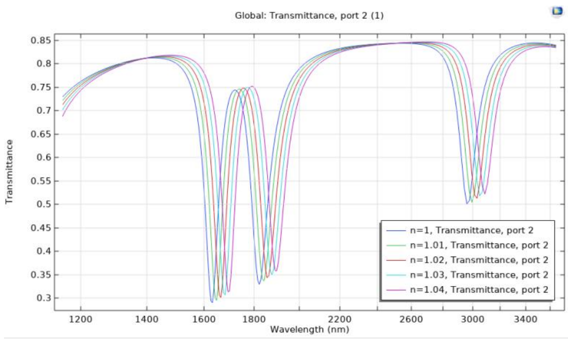
(c)	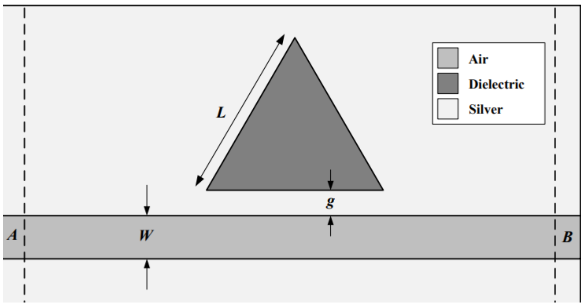	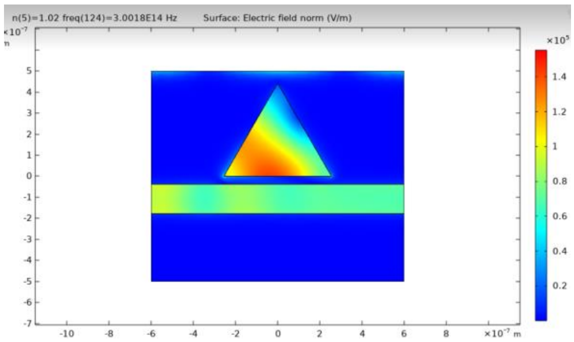
(d)	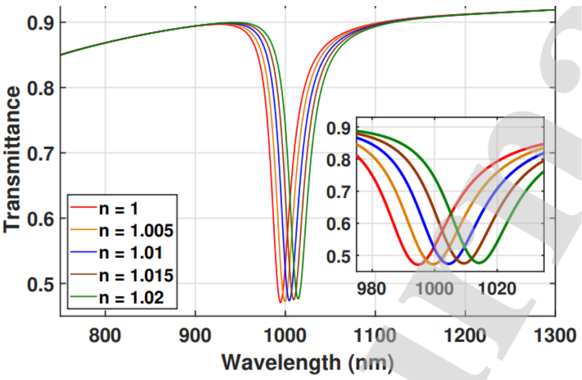	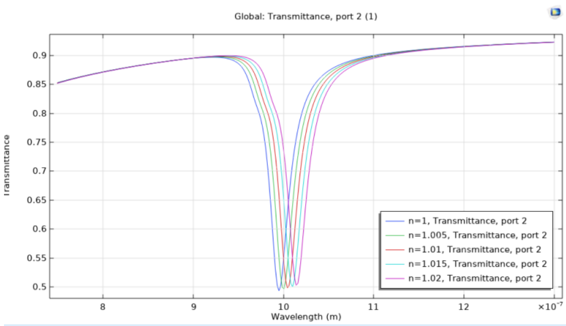

Figure 2.2: Comparison between Original figures and Resimulated results (a) Comparison between original figure of Plasmonic RI sensor [4] and resimulated figure (b) Comparison between transfer characteristics of RI sensor [4] and resimulated result (c) Comparison between original figure of RI Sensor Based on Triangular Resonator [5] and resimulated figure (d) Comparison between transfer characteristics of RI Sensor Based on Triangular Resonator [5] and resimulated result

The figures and the above table 2.1 demonstrate a comparison analysis between the initial findings from a number of different studies and the transmission characteristics that were determined from our simulations. The practical usability of these plasmonic RI sensors in a variety of sensing applications is supported by this validation. It is vital to overcome this constraint and objectively enhance the sensitivity of these sensors in order to improve the efficacy and effectiveness of lab-on-chip sensors. Additionally, it is necessary to improve the sensitivity of these sensors. The objective of these literature evaluations was to offer us useful insights into successful design and parameter settings, which we used in order to construct a highly effective refractive index sensor that is suited for a wide variety of applications.

Chapter 3

Methodology

3.1 Material Modeling for Plasmonic Sensors

Materials' characteristics, such as their refractive index (n) and relative permittivity (εr), become frequency-dependent at high frequencies. Several models, including the Lorentz, Drude, and Lorentz-Drude models, have been created to quantitatively represent this frequency dependency. These models provide a way to precisely characterise frequently used plasmonic materials, such as gold and silver. Their behavior is modelled using the relevant tabular values. The finite element approach is used in numerical simulation programmes such as COMSOL Multiphysics Software. It discretizes the system boundary into a triangular mesh and approximates the field inside that boundary. Scattering boundary conditions are used to simulate transparent boundaries for incoming and outgoing signals. Important quantities like transmittance and reflectance in two-port electromagnetic wave-based devices are then assessed using scattering parameters. Mode analysis and boundary mode analysis make it possible to compute parameters like the propagation constant and other related features, which allows for the prediction of the fundamental mode propagation.

3.1.1 Lorentz Model

The Lorentz material model, which is sometimes called the Lorentz-Oscillator model, explains a lot about how things behave in electromagnetic fields. This model is important for understanding how dielectric materials behave and is used in optics, electromagnetics, and condensed matter physics, among other fields. Particles or groups of particles inside a material can be shown as harmonic vibrations. This is the basic idea behind the Lorentz model. When an electromagnetic field comes in and hits these oscillators at their normal resonant frequencies, they have a complicated dielectric reaction. The model says that when an electric field is put on something, the way the charges are spread inside it goes back and forth around a stable point.

Atoms consist of a positively charged nucleus containing protons and neutrons, with the nucleus carrying a total charge of +eZ, where Z is the atomic number. Surrounding the nucleus are Z electrons in a neutral atom [17]. Based on the rules of quantum physics, these electrons are connected to the nucleus by Coulomb forces and move around it. Some electrons in atoms with higher atomic numbers are very close to the centre and move in a tight circle around it. These are called core electrons. Valence electrons are different types of electrons that fill larger orbits and have less net positive charge from the nucleus because core electrons shield them. This makes the Coulomb binding forces weaker. These valence electrons can be moved around more easily, which makes them a big part of how the atom responds to polarization [18-20].

The Lorentz model simplifies the atom's behavior using four main assumptions:

1. The core doesn't move at all because its mass is so much greater than the electron mass.
2. The model only looks at valence electrons and doesn't look at how core electrons behave.
3. There is a harmonic binding potential between the valence electrons and the core. According to Hooke's Law, there is a force equal to the shift that pushes these electrons back into balance. Hooke’s Law:

$$F = Kx \tag{3.1}$$

Here, K is the spring constant, which tells us how strong the force is that holds things together [21].

4. The atom's response is isotropic, meaning it reacts equally in all directions to the applied electric field, allowing the electron's position to be described as a scalar r(t) [21][24][25].

When an alternating electric field is applied, the electron behaves like a spring. The equation can describe the forces:

$$[F_{\text{acceleration}} + F_{\text{damping}} + F_{\text{restoration}} = F_{\text{ext}}] \tag{3.2}$$

This is expressed as:

$$[m\frac{\partial^2 x}{\partial t^2} + m\gamma\frac{\partial x}{\partial t} + m\omega_0^2 x = qE] \tag{3.3}$$

Applying Fourier analysis to this equation, we obtain:

$$[m(-j\omega)^2 x(\omega) + m\gamma(-j\omega)x(\omega) + m\omega_0^2 x(\omega) = qE(\omega)] \tag{3.4}$$

$$[-\omega^2 + \omega_0^2 - j\gamma\omega]x(\omega) = \frac{q}{m}E(\omega)] \tag{3.5}$$

Dipole Moment and Polarization [22]

The dipole moment μ is given by:

$$[\mu = qx(\omega) = \frac{q^2}{m}\frac{E(\omega)}{\omega_0^2 - \omega^2 - j\gamma\omega}] \tag{3.6}$$

The polarization P(ω), being the product of the number of dipoles and the dipole moment, is:

$$[P(\omega) = N\mu = N\frac{q^2}{m}\frac{E(\omega)}{\omega_0^2 - \omega^2 - j\gamma\omega}] \tag{3.7}$$

The general formula for polarization is:

$$[P = \epsilon_0\chi(\omega)E(\omega)] \tag{3.8}$$

Comparing the above equations, we get:

$$[\epsilon_0\chi(\omega)E(\omega) = N\frac{q^2}{m}\frac{E(\omega)}{\omega_0^2 - \omega^2 - j\gamma\omega}] \tag{3.9}$$

Thus, the susceptibility $\chi(\omega)$ is

$$[\chi(\omega) = N\frac{q^2}{m\epsilon_0}\frac{1}{\omega_0^2 - \omega^2 - j\gamma\omega}] \tag{3.10}$$

We also know that:

$$[\chi(\omega) = \epsilon_r(\omega) - 1] \tag{3.11}$$

So,

$$[\epsilon_r(\omega) - 1 = N\frac{q^2}{m\epsilon_0}\frac{1}{\omega_0^2 - \omega^2 - j\gamma\omega}] \tag{3.12}$$

Letting $(\frac{Nq^2}{\epsilon_0 m} = \omega_p^2)$, the plasma frequency be known, (3.13)

we derive:

$$\epsilon_r() = 1 + \frac{\omega_p^2}{\omega_0^2 - \omega^2 - j\gamma\omega} \tag{3.14}$$

Real and Imaginary Components of Permittivity

The real and imaginary parts of permittivity are:

$$[\epsilon_r'(\omega) = 1 + \frac{\omega_p^2(\omega_0^2 - \omega^2)}{(\omega_0^2 - \omega^2)^2 + \gamma^2\omega^2}] \tag{3.15}$$

$$[\epsilon_r''(\omega) = \frac{\omega_p^2\omega\gamma}{(\omega_0^2 - \omega^2)^2 + \gamma^2\omega^2}] \tag{3.16}$$

Graphical Representation and Material Properties [7][9]

Figure 3.1 illustrates the real and imaginary parts of permittivity with $(\omega_p = 2), (\omega_0 = 2), and(\gamma = 0.3)$

The real part ϵ′(ω) indicates the material's frequency-dependent behavior, while the imaginary part ϵ″(ω) accounts for energy loss or absorption.

The refractive index n (ω) and the complex propagation constant k (ω) are obtained from the dielectric function as follows:

$$[n(\omega) = \sqrt{\frac{1}{2}\left(\sqrt{\epsilon'(\omega)^2 + \epsilon''(\omega)^2} + \epsilon'(\omega)\right)}] \quad (3.17)$$

$$[k(\omega) = \sqrt{\frac{1}{2}\left(\sqrt{\epsilon'(\omega)^2 + \epsilon''(\omega)^2} - \epsilon'(\omega)\right)}] \quad (3.18)$$

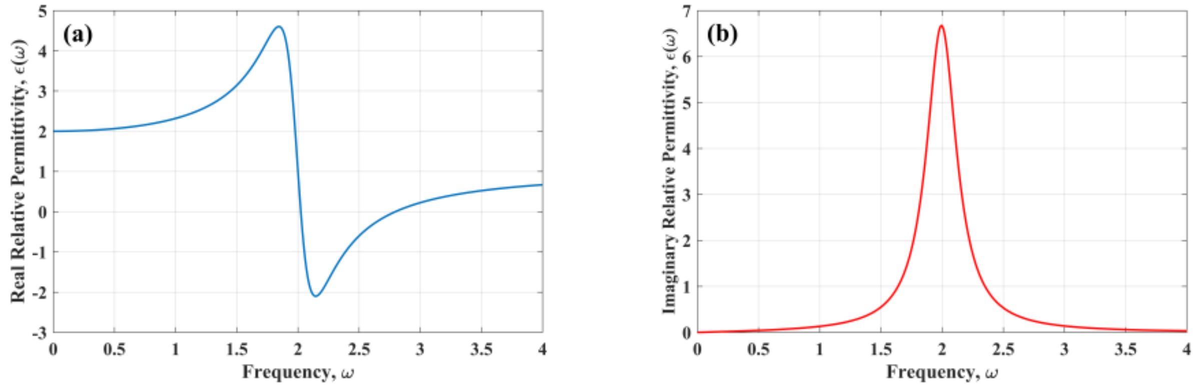

Figure 3.1: (a) The real part of permittivity ϵ′(ω) (b) The imaginary part of permittivity ϵ″(ω)

There are some limitations to the Lorentz Oscillator Model, as follows:

1. Applicability to Bound Electrons Only: The Lorentz model primarily describes the behavior of bound electrons in an atom, focusing on their oscillations around fixed positions. This makes the model inadequate for explaining the behavior of free electrons in metals, which are not bound to any specific atom and instead move freely through the material.

2. Neglect of Electron-Electron Interactions: The Lorentz model does not take into account the interactions between electrons themselves. In many materials, especially those with high electron densities, electron-electron interactions can significantly influence the optical and electrical properties, leading to deviations from the predictions of the Lorentz model.

3. Simplified Treatment of Damping: The damping term in the Lorentz model represents the loss of energy due to collisions and other dissipative processes. However, this treatment is overly simplified, assuming a constant damping rate for all electrons. In reality, damping can vary with frequency and other factors, making the model less accurate for materials with complex dissipation mechanisms.

4. Inaccurate for High-Frequency Phenomena: The Lorentz model is not well-suited for describing the optical properties of materials at high frequencies, such as in the ultraviolet or X-ray regions. It assumes a simple harmonic oscillator behavior, which does not capture the complexities of electronic transitions between different energy bands or the detailed electronic band structure of the material [25].

3.1.2 Drude Model

The Drude model, provides a classical framework for understanding the electrical and optical properties of metals and conductors when exposed to electromagnetic fields. This model simplifies the complex behavior of these materials, making it easier to study their conductivity and interaction with light. The Drude model treats conduction electrons in a metal as a gas of free electrons that move randomly and occasionally collide with fixed lattice ions. This approach allows us to describe the macroscopic current density (J) in terms of the applied electric field (E) using Ohm’s law:

$$J(t) = \sigma E(t) \tag{3.19}$$

Here, J(t) is the current density as a function of time, E(t) is the applied electric field, and σ is the electrical conductivity of the material [26]. A key concept in the Drude model is relaxation time (τ), which represents the average time between collisions of electrons. After each collision, an electron's velocity is assumed to become randomized, leading to an average net drift velocity of zero. The relaxation time is inversely proportional to the electron scattering rate and relates to the electrical conductivity as follows:

$$\sigma = \frac{ne^2\tau}{m} \tag{3.20}$$

In this equation, n is the number density of conduction electrons, e is the elementary charge, and m is the effective mass of the conduction electrons. In metals, most electrons are free and not tightly bound to atomic nuclei, meaning they do not experience significant restoring forces. Therefore, the natural frequency (ω_0) is negligible for metals. The Drude model can be derived from the Lorentz model by setting $\omega_0=0$, which reflects the absence of a characteristic natural frequency in metals [27]. This simplification allows us to focus on the collective behavior of free electrons in response to external fields, emphasizing their electrical conductivity and optical properties. The complex dielectric function $\varepsilon(\omega)$ of a diffuse material can be expressed as:

$$\varepsilon(\omega) = 1 - \frac{\omega_p^2}{\omega^2 + i\gamma\omega} \tag{3.21}$$

where ω_p is the plasma frequency, and γ is the collision frequency. The plasma frequency is given by:

$$\omega_p = \sqrt{\frac{ne^2}{\varepsilon_0 m}} \tag{3.22}$$

where ε_0 is the permittivity of free space.

The collision frequency γ is the reciprocal of the relaxation time:

$$\gamma = \frac{1}{\tau} \tag{3.23}$$

Real and Imaginary Parts of Permittivity

The real part (ε′(ω)) and imaginary part (ε″(ω)) of the dielectric function describe the material's dispersion and energy loss, respectively:

$$\varepsilon'(\omega) = 1 - \frac{\omega_p^2}{\omega^2+\gamma^2} \tag{3.24}$$

$$\varepsilon''(\omega) = \frac{\gamma\omega_p^2}{\omega(\omega^2+\gamma^2)} \tag{3.25}$$

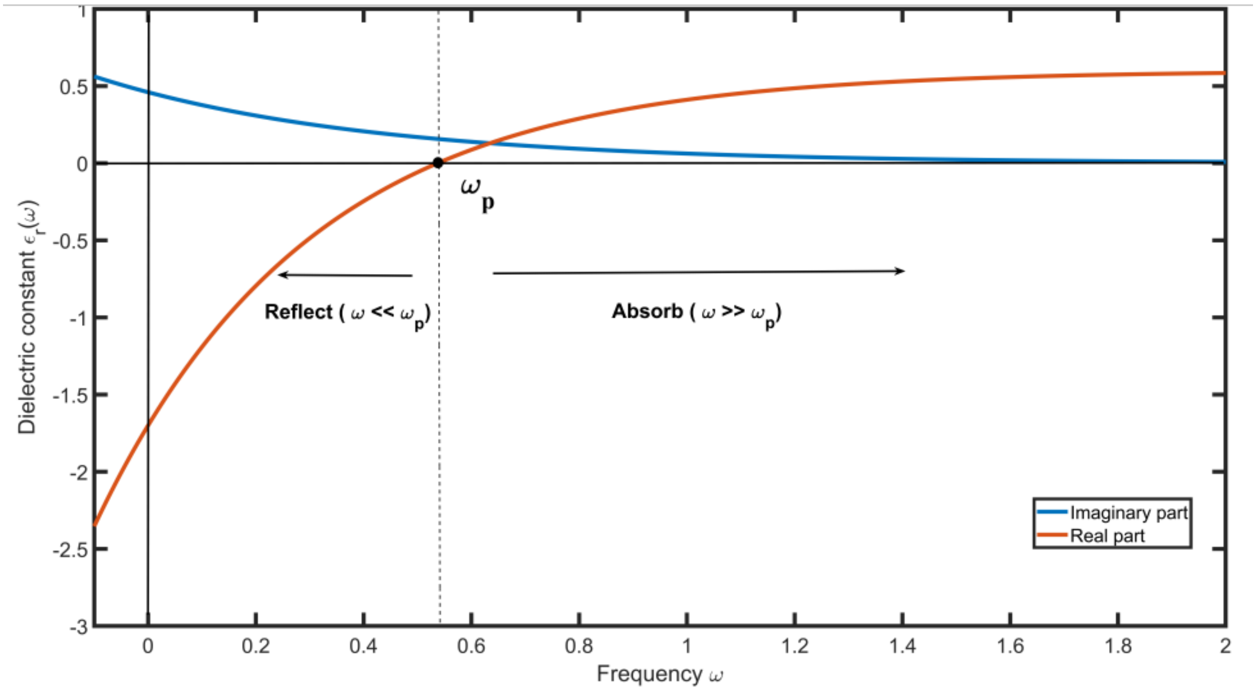

Figure 3.2: Real and Imaginary Part of Drude Model

Figure 3.2 demonstrates the the real part (ε′(ω)) and imaginary part (ε″(ω)) of the dielectric function. These expressions are crucial for understanding the frequency-dependent behavior of the material [28].

Optical Properties

The complex dielectric function allows us to derive important optical properties, such as the refractive index (n) and the propagation constant (k):

$$n(\omega) = \sqrt{\frac{1}{2}\left(\sqrt{\varepsilon'(\omega)^2 + \varepsilon''(\omega)^2} + \varepsilon'(\omega)\right)} \tag{3.26}$$

$$k(\omega) = \sqrt{\frac{1}{2}\left(\sqrt{\varepsilon'(\omega)^2 + \varepsilon''(\omega)^2} - \varepsilon'(\omega)\right)} \tag{3.27}$$

These properties help describe how light interacts with diffuse materials, affecting reflection, transmission, and absorption. In metals, the delocalized valence electrons can move freely, giving rise to electrical conductivity [29]. The plasma frequency (ωp) is directly related to this conductivity. Below ωp, metals are highly reflective due to the inability of incident photons to excite the conduction electrons, leading to the characteristic shiny appearance of metals.

Above ωp, metals become more transparent, with reduced reflectivity and increased light absorption. The Drude model is a powerful tool for understanding the electrical and optical behavior of metals and conductors. It simplifies complex interactions by focusing on free electron dynamics and provides a foundation for studying more advanced phenomena in material science and condensed matter physics [27-30].

Limitations of Drude Model:

1. Application to Free Electrons Only: The Drude model ignores interactions between electrons and the atomic lattice, assuming that conduction electrons in a metal behave as a free electron gas. This rough approximation doesn't do a good job of describing how bound electrons or electrons in complicated materials behave. As a result, predictions for materials with strong electron-lattice interactions are wrong. It is only effective for free electrons [7][9].

2. Simplified Collision Mechanism: Assuming that every collision totally randomizes the electron's velocity, the relaxation time (τ) in the Drude model represents the average interval between electron collisions. This oversimplification leaves out complex scattering mechanisms that happen in real materials, like impurity scattering, anisotropic scattering, and electron-phonon interactions, which leads to a too simple understanding of how electrons move.

4. Inaccurate optical characteristics: Although the Drude model offers a fundamental foundation for comprehending metals' optical characteristics, it is unable to predict materials' behavior at high frequencies, such as those found in the ultraviolet or X-ray spectrum. The model fails to take into account the precise band structure of the material and inter-band transitions, which causes significant discrepancies between experimental results and theoretical predictions in these regimes [29].

Because of the limitations of the Drude and Lorentz models—such as the Drude model's applicability only to free electrons and the Lorentz model's focus on bound electrons—neither model alone can fully describe the behavior of materials under all conditions. To address these limitations, the combined Drude-Lorentz model has been utilized in plasmonic sensors. This hybrid approach leverages the strengths of both models, providing a more comprehensive framework for understanding and designing advanced optical and electronic materials [30].

3.1.3 Drude-Lorentz Model

The Lorentz-Drude model is a sophisticated approach used to describe the behavior of conductors and metals under electromagnetic fields. While the Drude model offers a classical framework for understanding electrical conductivity and optical properties by treating conduction electrons as free electron gases, it falls short in capturing the nuanced frequency-dependent behavior of real materials. To overcome this, the Lorentz-Drude model integrates elements from both the Drude and Lorentz models, providing a more comprehensive picture that aligns well with experimental observations [31].

The Lorentz-Drude model builds upon the Drude model by incorporating the interactions between electrons and the resonant behavior of bound electrons. This dual approach allows it to account for the frequency-dependent dielectric response of materials, which is crucial for understanding their optical properties over a wide range of frequencies. The model is expressed mathematically by combining the Drude term, which accounts for free electron behavior, with Lorentz oscillators that represent bound electron contributions. The general expression for the electric displacement field D (ω) in the frequency domain is:

$$D(\omega) = \epsilon_0 \left[1 - \frac{\omega_p^2}{\omega^2 + i\omega\Gamma_0} + \sum_{j=1}^{k} \frac{f_j \omega_p^2}{\omega_j^2 - \omega^2 + i\omega\Gamma_j}\right] E(\omega) \tag{3.28}$$

Where ϵ0 is the vacuum permittivity, ωp is the plasma frequency of free electrons, and Γ0 is the damping factor for free electrons, ω is the angular frequency of the applied field, ωj is the resonance frequency of the j-th oscillator, fj is the oscillator strength of the j-th oscillator, Γj is the damping frequency of the j-th oscillator, and, E(ω) is the electric field in the frequency domain [7][9].

Real and Imaginary Parts of the Dielectric Function

The dielectric constant ϵr(ω) can be separated into its real and imaginary components to describe dispersion and absorption properties, respectively:

$$\varepsilon_r(\omega) = 1 - \frac{w_p^2}{\omega(\omega - i\Gamma_0)} + \sum_{j=1}^{k} \frac{f_j w_p^2}{(\omega_j^2 - \omega^2) + i\omega\Gamma_j} \tag{3.29}$$

Here, Ωp represents the plasma frequency of free electrons, distinguishing it from the collective plasma frequency ωp.

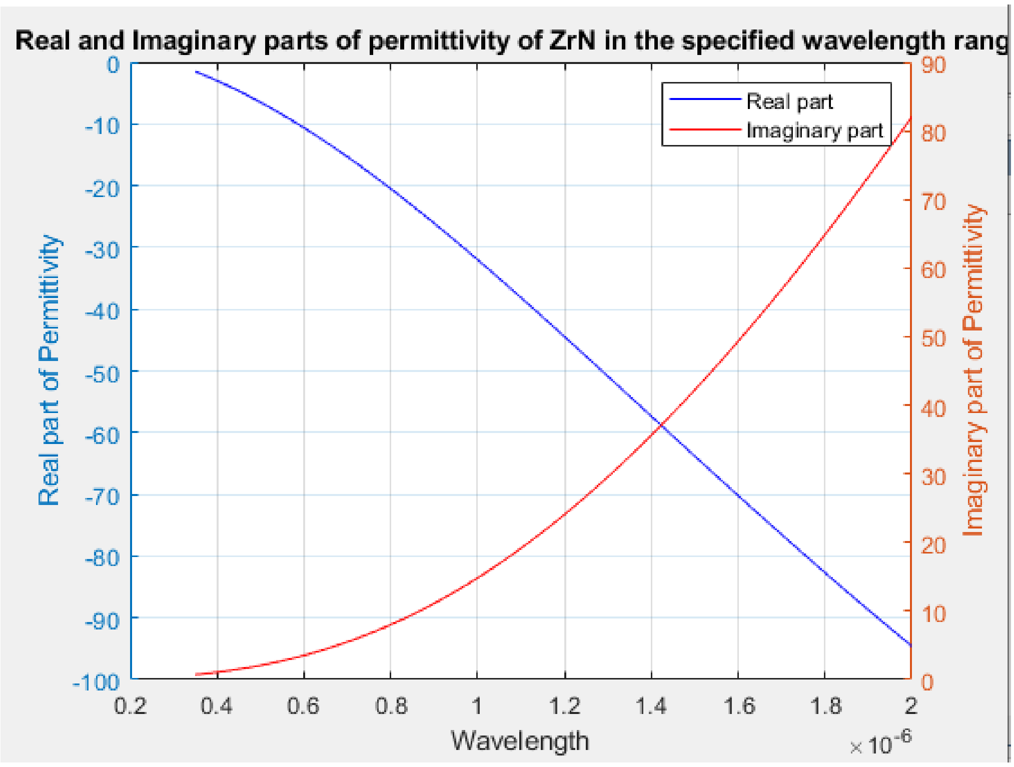

Figure 3.3: Real and Imaginary part of ZrN by utilizing Drude-Lorentz Formulation [7][9]

Key Aspects of the Lorentz-Drude Model

1. Frequency-Dependent Dielectric Response: The Lorentz-Drude model does a good job of capturing the frequency-dependent dielectric response by using damping coefficients and resonance frequencies. This allows for a realistic representation of how materials interact with electromagnetic fields across various frequencies.

2. Damping Effects: The model includes damping coefficients that account for energy dissipation and absorption processes. This is crucial for accurately describing how electromagnetic waves attenuate as they pass through a material [31].

3. Electron-Electron Interactions: By considering interactions between electrons, the model can describe collective electron behaviors such as plasmon resonances. These resonances are pivotal for understanding the optical properties of metals and conductors.

The Lorentz-Drude model is particularly valuable for designing and characterizing materials with tailored optical properties for applications in photonics, optoelectronics, and plasmonics. It provides insights into phenomena like plasmonic resonances, which are essential for developing advanced sensors and devices. The Lorentz-Drude model builds on the classical Drude model by adding bound electron effects and electron interactions. It provides a more accurate and complete way to study the electrical and optical properties of metals and conductors. This model has proven effective in predicting experimental outcomes and remains a cornerstone in the field of material science.

3.1.4 Finite Element Method (FEM)

In the physical sciences and engineering, the Finite Element Method (FEM) is a potent computational method used to resolve challenging issues. It entails breaking down a big, complicated system into smaller, easier-to-manage components called finite elements. After that, each of these components is examined separately, and their behaviors are integrated to provide a thorough understanding of the system as a whole. FEM is frequently utilized because of its adaptability and capacity to handle complicated geometries and boundary conditions in a variety of domains, including structural analysis, fluid dynamics, heat transfer, and electromagnetism. With the use of FEM, engineers and scientists can now precisely model, simulate, and evaluate systems for use in both academic and industrial settings. The discretization process, which splits a problem's continuous domain into a finite number of subdomains, or elements, is the fundamental step in the discretization process of FEM. These elements can take on several shapes based on the geometry of the problem and the required accuracy, including triangles, quadrilaterals, tetrahedrons, and hexahedrons. Every element has connections to its neighbours at points called nodes, and differential equations that are approximated by interpolation functions—often referred to as form functions—describe each element's physical behavior. Usually, polynomials that change among the elements enable the approach to accurately simulate the behavior of the physical system [32-35].

The creation of the system's governing equations is one of the most important phases in FEM. These equations, for example, are derived from the principles of equilibrium, compatibility, and material behavior in structural analysis. Using methods like the Galerkin method, the differential equations governing the physical phenomenon are converted into a set of algebraic equations. This conversion procedure, called the weak formulation, guarantees average satisfaction of the original differential equations over all finite elements. The flexibility of FEM includes its capacity to manage intricate material behaviors and nonlinearities. Nonlinear features of materials, including plasticity, hyperelasticity, or viscoelasticity, are frequently seen in real-world applications and can be included in FEM models. In nonlinear finite element modelling (FEM), updating the geometry and material properties is done by solving systems of equations over and over again until convergence is reached. Because of this feature, FEM is an effective tool for investigating nonlinear processes, contact mechanics, and problems involving massive deformations [33].

Strong numerical methods are employed in the analysis and resolution of intricate engineering and physical issues through the use of the finite element method (FEM). There are typically four primary steps in the process:

1. Determination of the Solution Boundary: The first phase in the field element method (FEM) is to divide the whole problem domain (also referred to as the solution domain) into more manageable, smaller subdomains called elements. We refer to this procedure as discretization, or meshing. If you were to study a large sheet of paper in depth, you would cut it into tiny pieces so that you could look more closely at each area. Through this process, we are able to convert a continuous problem—which is frequently too complicated to answer directly—into a discrete problem that can be solved numerically.

2. Derivation of Equations: The governing equations for a typical element are then derived after the domain has been partitioned into its constituent elements. The Navier-Stokes equations for fluid dynamics, Newton's laws for mechanical issues, and the heat equation for thermal analysis are examples of the physical laws that serve as the foundation for these equations. In essence, we examine each component's behavior in relation to the governing physical laws. For instance, we may determine how heat moves through each minuscule portion of the material via a thermal analysis [34].

3. Integration of Component Formulas: Equations for each individual element must be derived, and then they must be put together into a thorough system of equations that covers the whole domain. This process is known as the assembly of elemental equations. In this stage, all of the individual element equations are combined while accounting for the interactions between adjacent elements. It's similar to assembling a jigsaw puzzle in which every component fits together to form the whole image. We can build a comprehensive mathematical model that explains the behavior of the entire system by putting these equations together.

4. Solution of the Equations: In order to determine the numerical solution to our problem, the system of equations must be solved as the last step. To solve the equations and get the required answers, this entails applying a variety of numerical approaches. Different approaches, such as Gaussian elimination for smaller systems or iterative techniques like the conjugate gradient method for bigger, more complicated systems, may be utilized, depending on the size and complexity of the system. The required level of precision and the available computational power determine which approach is best.

With the help of these procedures, scientists and engineers may apply FEM to examine a variety of intricate physical phenomena and derive numerical solutions that offer insightful information about how various systems behave.

By using the finite element method, it is possible to discretize the Laplace equation's domain and solve the resulting system of equations to approximate the field potential V. This gives us insights into the distribution of potential over the domain, which is important for many scientific and engineering applications. We may address issues in a variety of domains, such as electrostatics, heat conduction, and fluid flow, by using FEM to solve Laplace's equation. This allows us to comprehend the steady-state distribution of the field potential in the absence of sources or time-varying phenomena on a deeper level.

To provide a concrete example, let's look at the generalized wave equation provided by:

$$\nabla^2 V + k^2 V = g \tag{3.30}$$

Here, k is the medium's wavenumber, g is the source term, and V stands for the unknown field potential that needs to be found [36]. We can examine a particular instance known as Laplace's equation, which is expressed as follows, in order to simplify our issue:

$$\nabla^2 V = 0 \tag{3.31}$$

Since k=g=0, there are no outside sources or wave propagation effects. According to Laplace's equation, a steady-state situation is one in which the field potential V is constant over time. In electrostatics, for example, where we might be interested in the electric potential in a charge-free region; in heat conduction, where we want to find the temperature distribution in a material without internal heat generation; and in fluid flow, where we might be looking at the potential flow in a region without any fluid sources or sinks, this is helpful for solving problems where there are no sources or sinks within the domain [37].

Chapter 4

Sensor Design, Optimization, and Applications

4.1 Structure Design and Parameter Settings

The top view of the initially proposed structure has been illustrated in a two-dimensional (2D) diagram in Fig. 4.1. Refractive index sensing depends on the light-matter interaction between the waveguide and the material being sensed. Table 4.1 provides the details of the geometric parameters used in designing the sensor. Typically, silver is employed for refractive index sensing due to its higher sensitivity compared to other metals.

The numerical simulation is executed using COMSOL Multiphysics 5.6 software. As the width of the waveguide is much smaller than the incident wavelength, other modes cannot propagate or be sustained in the waveguide, and the waveguide can only support the most fundamental transverse magnetic (TM) mode. Surface plasmon polaritons (SPPs) are excited in TM mode from the input port A in Fig. 4.1.

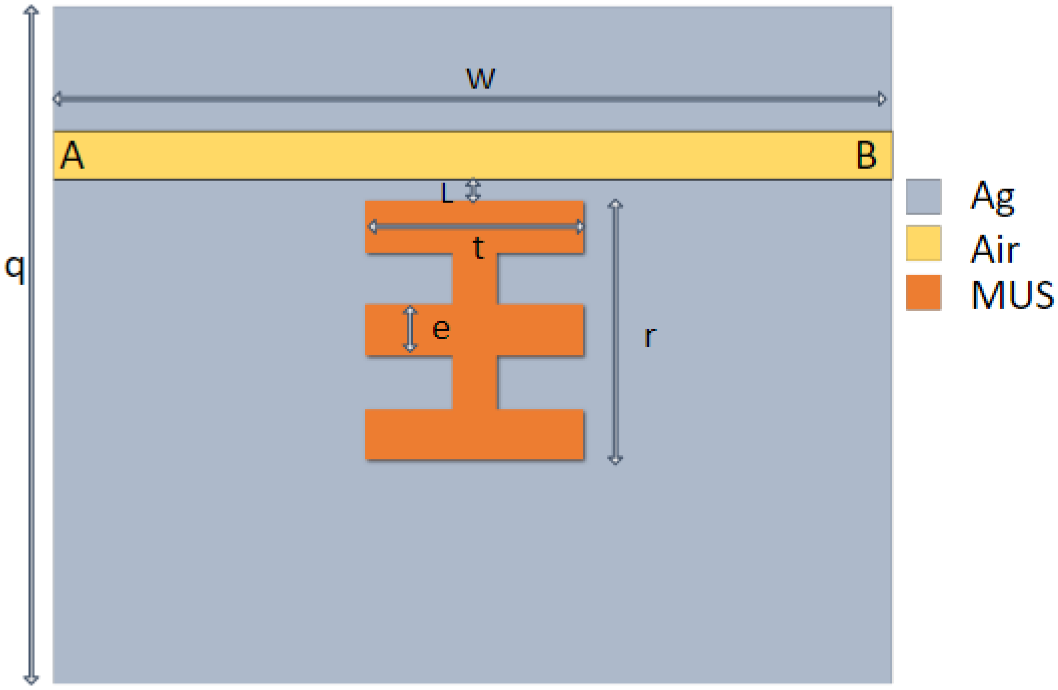

Figure 4.1: Structure of our Proposed RI Sensor

Name of the Parameter	Symbol	Value (nm)
Rectangle Length	q	1000
Rectangle Width	w	800
Small Height	e	48
Length of MUS	r	280
Width of MUS	t	200
Refractive Index	n	1
Minimum Value of Wavelength	λ1	550
Maximum Value of Wavelength	λ2	2500
Distance between Waveguides	L	50

Table 4.1: Parameter Values of the sensor at the initial stage

From figure 4.1, it is evident that we designed a refractive index (RI) sensor using a straight waveguide made of air, starting from port A and ending at port B. Silver (Ag) was chosen initially as the metal for the waveguide due to its higher sensitivity compared to other metals like gold, making it ideal for RI sensing applications. Silver's superior plasmonic properties allow for enhanced light-matter interaction, leading to more accurate and sensitive detection of RI changes. The material under sensing (MUS) is crucial, as it is the region where the RI variations will be detected, allowing us to measure changes in the surrounding medium's refractive index accurately [36].

The parameter values and materials used in the design are detailed in Figure 4.1 and Table 4.1. A rectangle length (q) of 1000 nm defines the overall length of the sensor structure. A rectangle width (w) of 800 nm determines the width of the air waveguide. A small height (e) of 48 nm specifies the height of the MUS, which is critical for ensuring effective light interaction within the sensor. A length (r) of 280 nm and a width (t) of 200 nm for the MUS, provide the dimensions for the material where the refractive index variations will be sensed. A refractive index (n) of 1 for the material within the waveguide, representing the baseline medium. To cover a specific spectral range, we have taken the minimum value of the wavelength ($\lambda 1$) as 550 nm and the maximum value of the wavelength ($\lambda 2$) as 2500 nm. This range is chosen to ensure that the sensor can operate effectively across a wide range of light frequencies, enhancing its applicability in various sensing environments. The distance between the waveguides (L) is 50 nm, which is a crucial parameter to ensure proper coupling and interaction between the waveguides and the sensing material.

These parameter values will go through various changes in simulations to find the optimized result, ensuring that the sensor performs efficiently across the specified wavelength range of 550 nm to 2500 nm. By adjusting these parameters, we aim to achieve the best possible sensitivity and accuracy for the RI sensor. The use of MUS allows us to effectively sense and measure the RI variations, making our design suitable for a wide range of sensing applications. The parameters and materials mentioned provide a solid foundation for the sensor's operation, ensuring accurate and reliable RI measurements. Because of silver's plasmonic properties, the precise geometric parameters, and the wide wavelength range, the sensor can pick up on even small changes in the refractive index. This makes it a useful tool for many optical sensing tasks.

In order to eliminate interference in the simulated results and produce valid data, the scattering boundary condition in the simulation setup absorbs the outgoing waves and avoids undesired reflections. The simulation is divided into finer-grained components through the use of extra-fine triangular meshing, which increases the simulation's resolution and accuracy. This framework applies the finite element technique (FEM) for the numerical solution of the electromagnetic wave equations with material interfaces. Partial differential equations (PDEs) can be solved using FEM, which simplifies the solution domain into discrete, basic components. This approach mimics the way waves behave when they interact with various materials and allows for a thorough investigation of complicated systems [37].

In materials science, the Lorentz-Drude model is frequently used to study metal behavior at the atomic and molecular levels. It offers a helpful theoretical framework to analyze the structural features of metals, including their optical response and electronic structure. Through a series of equations that account for the effects of electron collisions with the metal's lattice vibrations, the model depicts the behavior of electrons. Eq. 4.1 represents the complex dielectric function, which is a crucial parameter that can be computed thanks to the Lorentz-Drude model. It describes how a material reacts to electromagnetic radiation at different frequencies by taking into account two types of electrons: bound and free electrons. Eq. 4.2 represents the response of the free electrons, which can be explained by the Drude model, and Eq. 4.3 represents the response of the bound electrons, which can be explained by the Lorentz model. The material's capacity to retain energy in the presence of an electric field is characterized by the real part, while its capacity to release energy is described by the imaginary part [38].

The formulation of the complex dielectric function, $(\hat{\varepsilon}_r(\omega))$ considering both free and bound electrons, is given by:

$$\hat{\varepsilon}_r(\omega) = \hat{\varepsilon}_r^{(f)}(\omega) + \hat{\varepsilon}_r^{(b)}(\omega) \tag{4.1}$$

The contribution from the free electrons, described by the Drude model, is:

$$\hat{\varepsilon}_r^{(f)}(\omega) = 1 - \frac{w_p^2}{\omega(\omega - i\Gamma_0)} \tag{4.2}$$

The contribution from the bound electrons [7][9], described by the Lorentz model, is:

$$\hat{\varepsilon}_r^{(b)}(\omega) = \sum_{j=1}^{k} \frac{f_j \omega_p^2}{\omega_j^2 - \omega^2 + i\omega\Gamma_j} \tag{4.3}$$

4.2 Parameter Variations and Sensitivity Analysis

In the process of designing our RI sensor, we systematically varied different parameters to perform a comprehensive sensitivity analysis and determine the optimal values for achieving the highest performance. Sensitivity analysis involves evaluating how changes in parameter values affect the sensor's ability to detect variations in the refractive index. Specifically, we analyzed the sensitivity of the sensor by calculating the shift in the resonance wavelength (Δλ) in response to changes in the refractive index (Δn). The sensitivity (S) can be formulated as:

$$S = \frac{\Delta\lambda}{\Delta n} \tag{4.4}$$

where Δλ represents the change in the resonance wavelength, and Δn is the change in the refractive index. By changing things like the waveguide's width, the MUS's length, and the space between waveguides, we tested how these changes affected the resonance wavelength shift and found the best configurations for sensitivity [37-40].

4.2.1 Variations of width (t) of MUS

We conducted a detailed sensitivity analysis by varying the parameter t, which represents the width of the MUS. The values of t were varied across a range of 180 nm, 200 nm, 220 nm, 230 nm, and 250 nm. Figure 4.2 demonstrates the transmission characteristics for these five different values of t. Through this analysis, we observed how changes in the width of the MUS influenced the sensor's performance. It was found that as t increased, the sensitivity of the sensor also increased, reaching an optimal value at t = 250 nm. This optimized value gave the biggest change in resonance wavelength for a given change in the refractive index. This made it easier for the sensor to accurately detect changes in RI.

The optimization process highlighted the importance of the MUS width in determining the overall performance of the sensor. By fine-tuning t to 250 nm, we achieved the best possible configuration, ensuring that the sensor operates with high sensitivity and reliability. This optimized parameter, along with the other design considerations, enables our RI sensor to perform effectively across a wide range of applications, providing accurate and sensitive measurements of refractive index changes.

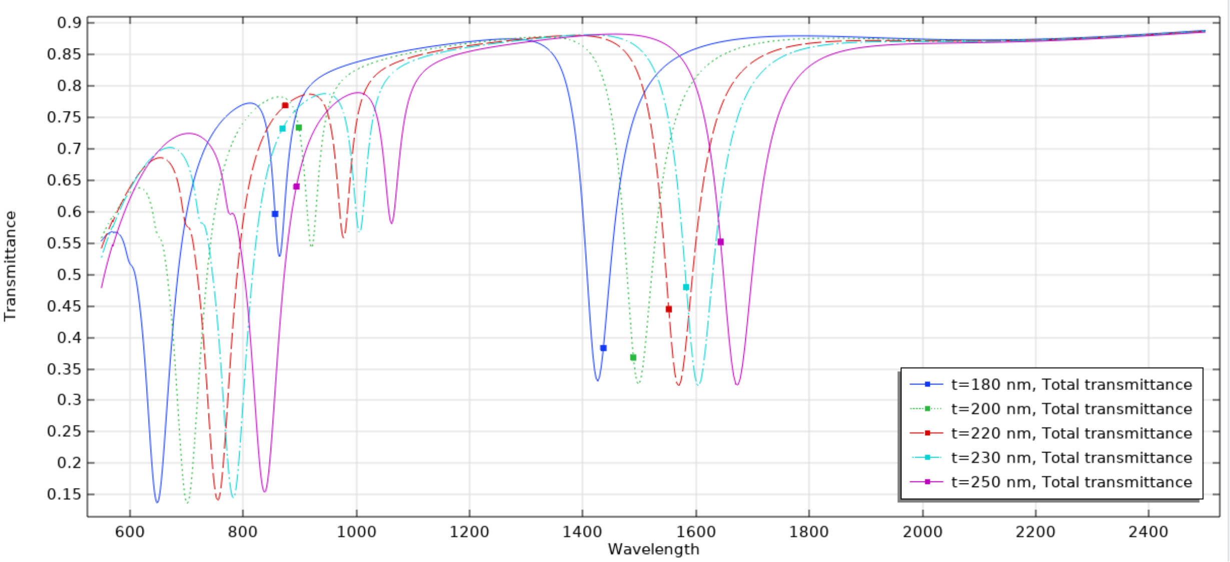

Figure 4.2: Transmittance characteristics for different values t

4.2.2 Variations of small height (e) of MUS

We conducted a detailed sensitivity analysis by varying the parameter e, which represents the small height of the MUS. The values of e were varied across a range of 45 nm, 48 nm, 52 nm, 55 nm, and 60 nm. Through this analysis, we observed how changes in the small height of the MUS influenced the sensor's performance. It was found that as e increased, the sensitivity of the sensor also increased, reaching an optimal value at e = 55. This optimized value provided the highest resonance wavelength shift for a given change in the refractive index, thereby maximizing the sensor's ability to detect RI variations accurately.

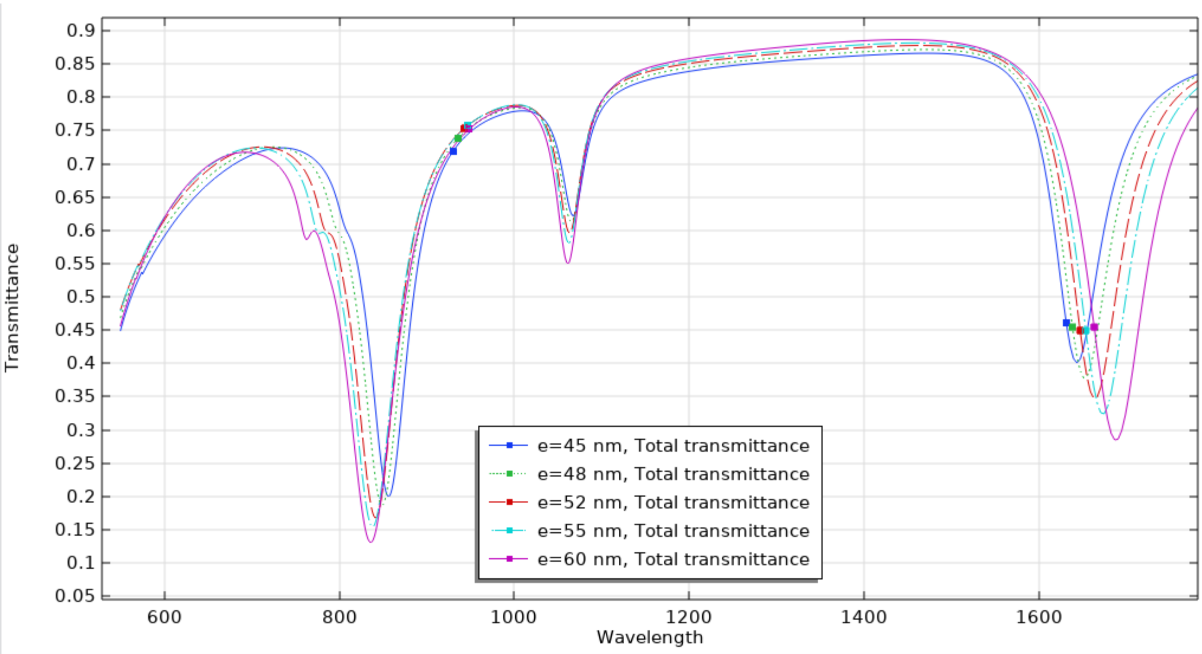

Figure 4.3: Transmittance characteristics for different values e

Figure 4.3 demonstrates the transmission characteristics for these five different values of e. The optimization process highlighted the importance of the small height of the MUS in determining the overall performance of the sensor. By fine-tuning e to 55 nm, we achieved the best possible configuration, ensuring that the sensor operates with high sensitivity and reliability. This optimized parameter, along with other design considerations, enables our RI sensor to perform effectively across a wide range of applications, providing accurate and sensitive measurements of refractive index changes.

4.2.3 Variations of Refractive Index (*n*)

We conducted a detailed sensitivity analysis by varying the refractive index from 1.0, 1.1, 1.2, 1.3, 1.4, and 1.5. Through this analysis, we observed how changes in the refractive index influenced the sensor's performance. It was found that as the refractive index increased, the sensitivity of the sensor also increased, with the highest sensitivity achieved at mode 3. This optimal mode provided the greatest resonance wavelength shift for a given change in the refractive index, thereby maximizing the sensor's ability to detect RI variations accurately. Figure 4.4 demonstrates the transmission characteristics for these different refractive indexes.

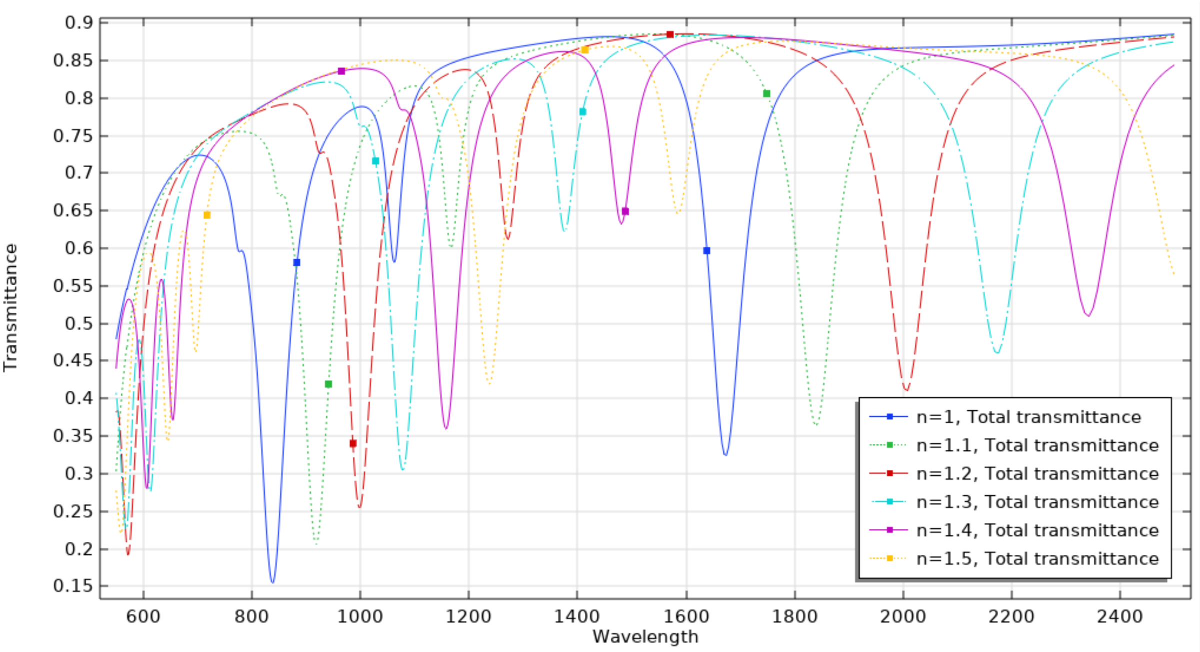

Figure 4.4: Transmittance characteristics for different values, *n*

Next, we took the values of refractive index and wavelength from mode 3 and plotted them using MATLAB. By employing MATLAB coding, we aimed to prove the linearity between resonance wavelength and refractive index [7][40]. This involved creating a plot that displayed the relationship between the refractive index and the resonance wavelength, thereby demonstrating how changes in one variable affect the other.

In Figure 4.5, we obtained a linear straight line from the RI vs. resonance wavelength graph, confirming the linearity of the relationship. This linearity is crucial, as it proves that our sensor can reliably detect changes in the refractive index with a consistent and predictable response. The linear graph validates our sensitivity analysis and ensures that the sensor performs accurately across a wide range of refractive index values, making it suitable for various applications.

Figure 4.5: Linear Straight line from Resonance Wavelength Vs Refractive index graph

4.3 Alternative Material, ZrN

One of the main focuses of our thesis was to explore alternative materials, like ZrN for use in our RI sensor. The choice of material is crucial, as it significantly affects the sensor's performance, especially in terms of compatibility, stability, and resistance to various factors. Silver, commonly used in such applications, presents several disadvantages that necessitate the search for better alternatives [7].

Disadvantages of Silver

1. Incompatibility with CMOS Technologies: Silver is not compatible with CMOS (Complementary Metal-Oxide-Semiconductor) technologies, which are widely used in the semiconductor industry for constructing integrated circuits. Because of this, silver-based parts can't be used in modern semiconductor devices because they don't work with them. This limits their use in advanced electronic and optical systems.

2. Tarnished Layer Due to Oxidation: Silver tends to form a tarnished layer because of oxidation when exposed to air. This oxidation process degrades the optical properties of silver, such as its reflectivity and conductivity, which can adversely affect the performance and longevity of sensors that rely on these properties.

Advantages of ZrN over Silver

1. CMOS Compatibility: ZrN (Zirconium Nitride) is fully compatible with CMOS technologies, making it suitable for integration with modern semiconductor devices. This compatibility ensures that ZrN can be easily incorporated into existing manufacturing processes, enhancing the versatility and applicability of ZrN-based sensors in the semiconductor industry.

2. Better Corrosion Resistance: ZrN exhibits superior corrosion resistance compared to silver. This enhanced resistance ensures that ZrN-based sensors maintain their performance and reliability over longer periods, even in harsh environmental conditions. This property is particularly important for applications where the sensor is exposed to corrosive substances or extreme conditions.

3. Thermal Stability at High Temperatures: ZrN maintains its stability at high temperatures, which is essential for applications involving elevated thermal conditions. This thermal stability ensures that the sensor's performance remains consistent and reliable, even in environments with significant temperature fluctuations.

4. Low Electrical Resistance: ZrN has lower electrical resistance, which can contribute to improved performance in electronic and optical devices. Lower resistance means that ZrN-based sensors can operate more efficiently, with less energy loss and better signal transmission.

5. High Hardness: The high hardness of ZrN makes it more durable and resistant to physical wear and tear. This durability ensures that ZrN-based sensors can withstand mechanical stresses and maintain their functionality over extended periods, reducing the need for frequent maintenance or replacement [7].

In our study, we replaced silver with ZrN as the metal in our RI sensor. Figure 4.6 demonstrates the use of ZrN in place of silver, highlighting its advantages and how it impacts the overall performance of the sensor.

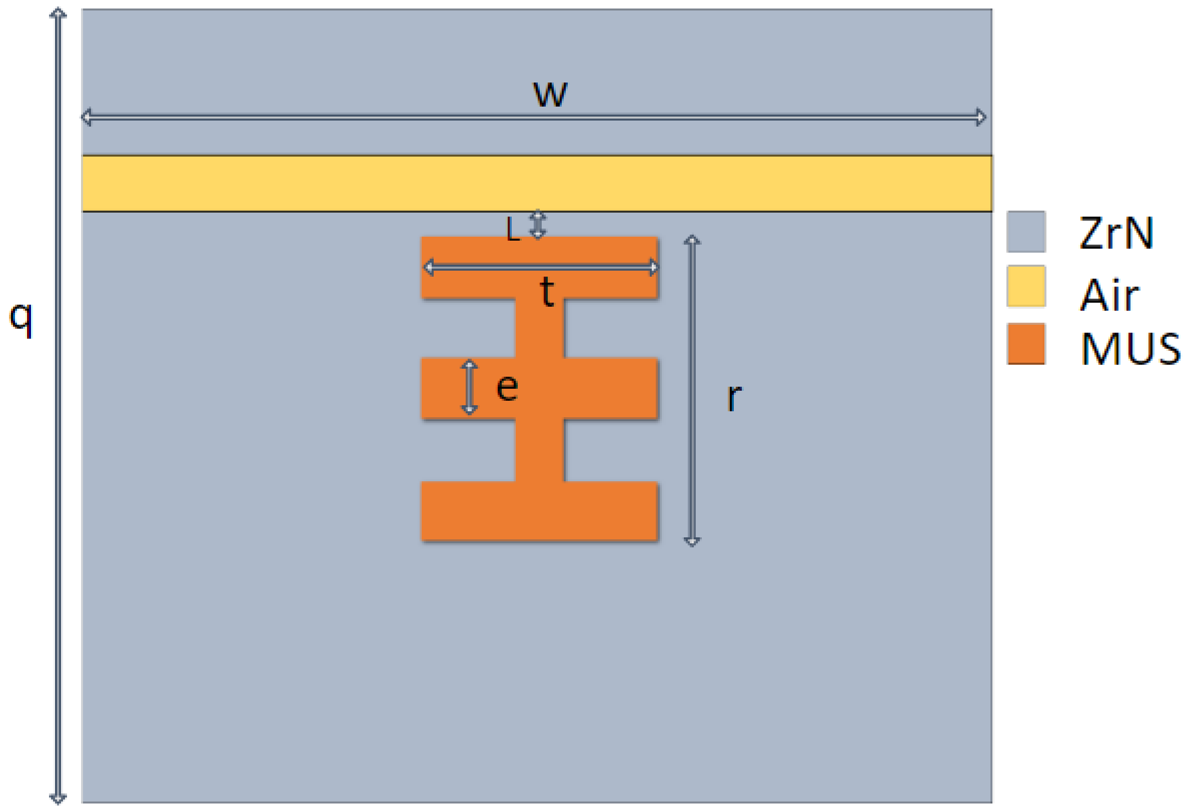

Figure 4.6: Modified structure with ZrN Material

4.3.1 Utilization of the Drude-Lorentz Model

To understand the optical properties of ZrN, we employed the Drude-Lorentz model [7]. The Drude-Lorentz model is widely used to describe the dielectric function of metals and provides a comprehensive understanding of their optical behavior. The equation of the Drude-Lorentz model is given as:

$$\varepsilon_r(\omega) = 1 - \frac{w_p^2}{\omega(\omega - i\Gamma_0)} + \sum_{i=1}^{k} \frac{f_j w_p^2}{(\omega_j^2 - \omega^2) + i\omega\Gamma_j} \tag{4.5}$$

From Equation 4.5, we derived the real and imaginary parts of the permittivity. By using MATLAB coding, we plotted these values to visually analyze the optical properties of ZrN. Figure 4.7 (a) demonstrates the real and imaginary parts of the permittivity of ZrN, showcasing how these components vary with frequency.

Utilizing the relationship for the refractive index:

$$n = \sqrt{\varepsilon} \tag{4.6}$$

We determined the real and imaginary parts of the refractive index separately. The real part of the refractive index corresponds to the phase velocity of light in the material, while the imaginary part represents the absorption loss [7]. Figure 4.7 (b) illustrates the real and imaginary parts of the refractive index of ZrN, obtained through MATLAB plotting.

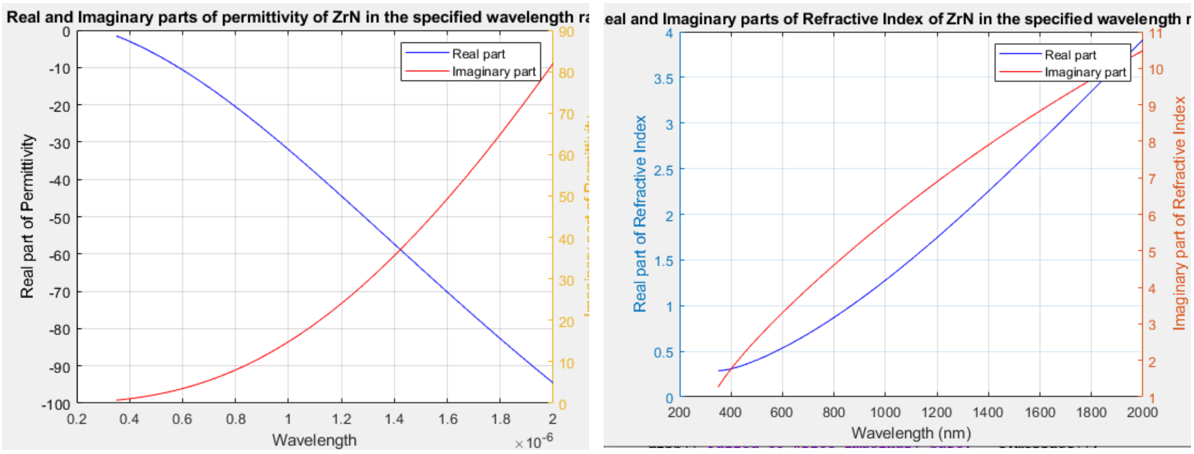

(a) (b)

Figure 4.7: (a) Real and Imaginary Parts of Permittivity of ZrN (b) Real and Imaginary Parts of Refractive Index of ZrN

By taking the real and imaginary parts of the refractive index derived from the Drude-Lorentz model, we were able to integrate them into COMSOL simulations. These simulations allowed us to predict and analyze the transmission characteristics of ZrN-based sensors accurately. The parametric sweep and parameter analysis facilitated a comprehensive understanding of how different parameters affect the transmission profile, ensuring that the sensor is optimized for maximum performance. Figure 4.8 presents the transmission characteristics obtained from these simulations, demonstrating the effectiveness of ZrN in enhancing the sensor's performance [9][10].

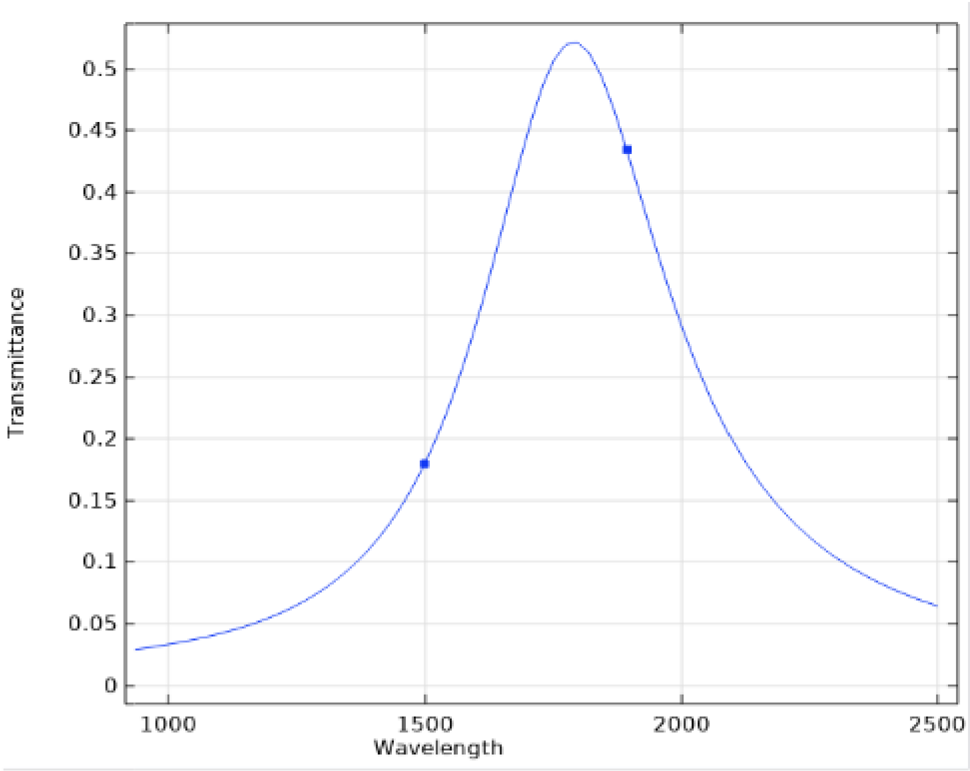

Figure 4.8: Transmission Characteristics of ZrN

4.4 Final Values after Optimization and Result Analysis

After the optimization process has been completed, the parameters that have been optimized are displayed in Table 4.2. These parameters correspond to the most efficient combination that results in the best possible outcome. The transmission spectra for the optimized parameters are depicted in Figure 4.9 according to the various values of the refractive index. The maximum sensitivity had been recorded at the value of 1650 nm/RIU. The distributions of the electric field for two different resonant modes are depicted in Figure 4.10 (a-b), while the distributions of the magnetic field for two different resonant modes are shown in Figure 4.10 (c-d).

Name of the Parameter	**Symbol**	**Value (nm)**
Rectangle Length	q	1000
Rectangle Width	w	800
Small Height	e	55
Length of MUS	r	280
Width of MUS	t	250

Refractive Index	n	1.1
Minimum Value of Wavelength	λ1	550
Maximum Value of Wavelength	λ2	2500
Distance between Waveguides	L	50

Table 4.2: Modified Parameter Values after Optimization

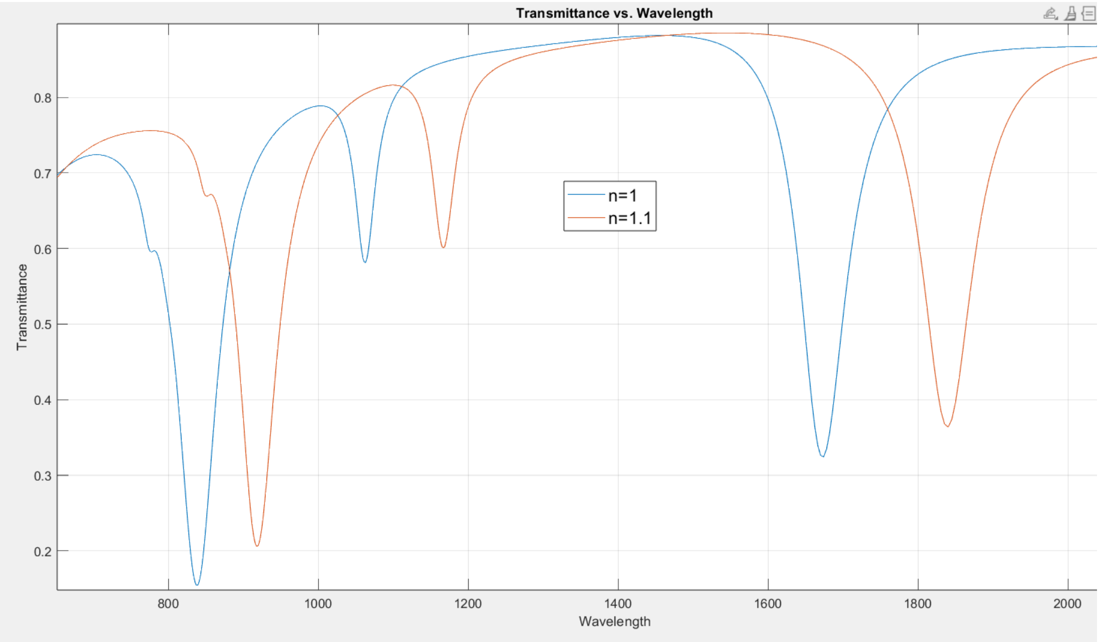

Figure 4.9: Final Tranmission Chracteristics

After conducting extensive parameter analysis, we obtained the final characteristics curve for our RI sensor. This optimization process was crucial in identifying the ideal parameters that maximize the sensor's performance. Through meticulous adjustments and sensitivity analyses, we ensured that the sensor operates with high accuracy and reliability.

We achieved electric field distribution (V/m) and magnetic field distribution (A/m) in our optimized sensor. These favorable distributions were observed at the maximum resonant peaks, indicating the sensor's enhanced performance. The figures illustrating the electric and magnetic field distributions reveal that the sensor effectively concentrates the fields at these resonant peaks, which is critical for accurate and sensitive detection of refractive index changes [40-42].

This clear and well-defined field distribution underscores the effectiveness of our optimization efforts and highlights the sensor's potential for high-precision applications.

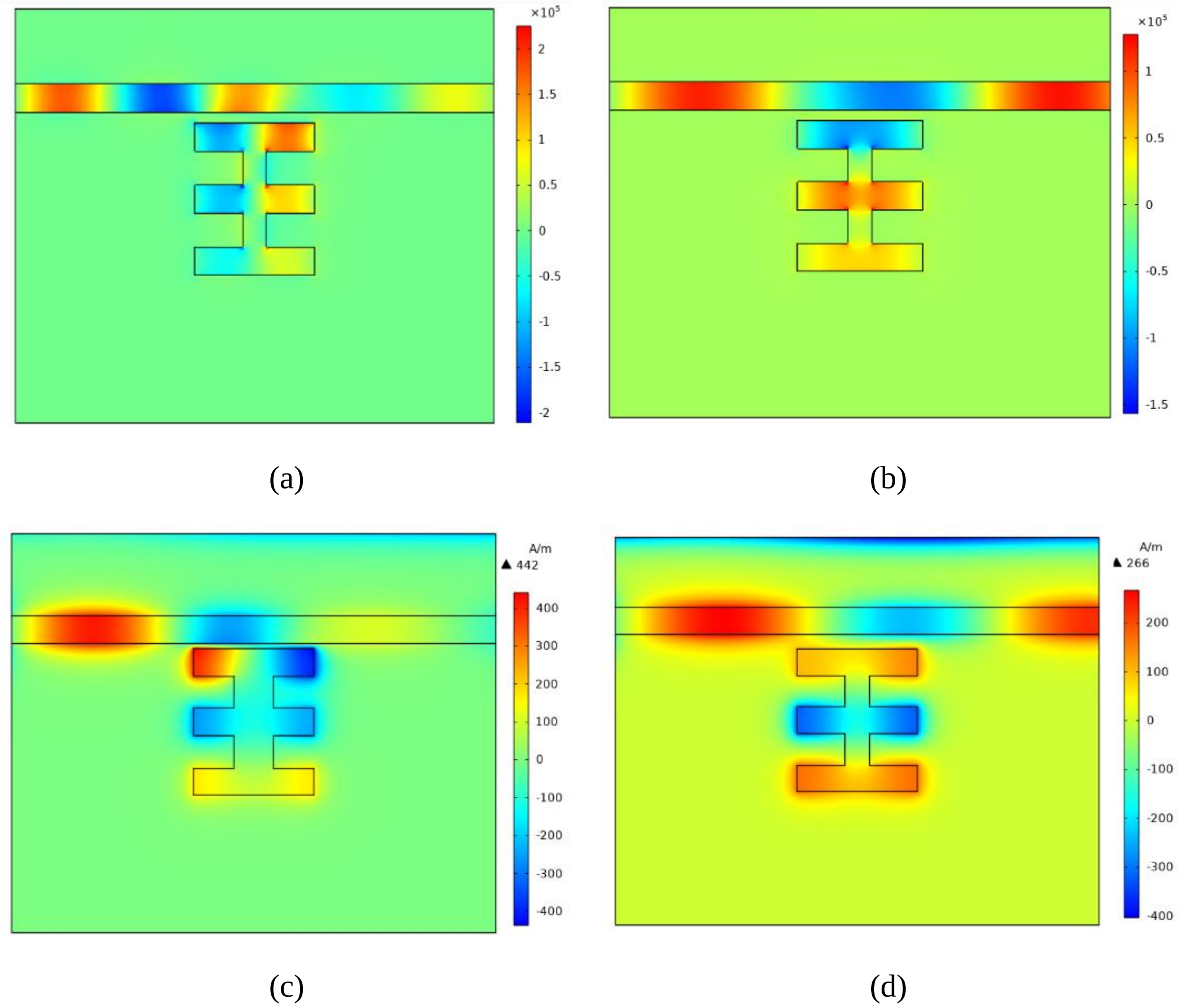

Figure 4.10: Electric field distribution (V/m) for n = 1.1 (a) resonant wavelength = 1030 nm (b) maximum resonant wavelength = 1650 nm and magnetic field distribution, Hz (A/m) for n = 1.1 (c) resonant wavelength = 1030 nm (d) maximum resonant wavelength = 1650 nm

4.5 Biosensing Applications

The optimized RI sensor, with its high sensitivity and reliability, has been utilized across various biosensing applications, demonstrating its versatility and effectiveness. This sensor's ability to accurately detect changes in the refractive index makes it beneficial for numerous biomedical applications. For instance, in diabetes severity detection, the sensor can measure glucose concentrations in biological fluids with high precision. Similarly, in anemia type detection, it can differentiate between various forms of anemia by analyzing the refractive index variations in blood samples. Moreover, the sensor's capability extends to cancer cell detection, where it can identify malignant cells based on their distinct refractive index properties compared to healthy cells. These applications showcase the sensor's potential for early diagnosis and monitoring of diseases, contributing to improved healthcare outcomes. The advanced sensitivity and specificity of our optimized RI sensor pave the way for its use in a wide range of clinical and research settings, offering a powerful tool for medical diagnostics [4][5].

4.5.1 Detection of Diabetes Severity

Blood glucose concentration refers to the amount of glucose present in a given volume of blood. Glucose is a critical energy source for the body, and its concentration in the blood is tightly regulated to maintain homeostasis. Blood glucose levels vary throughout the day, influenced by factors such as recent meals, age, and overall health. The glucose concentration percentage can be calculated using the following equation:

$$n = 0.2015 \times C\% + 1.3292 \tag{4.7}$$

where n represents the refractive index, and C% is the glucose concentration percentage [3]. This equation establishes a direct relationship between the refractive index and the glucose concentration, which can be utilized to determine the unknown concentration percentage of glucose. To convert glucose concentration from percentage to mmol/L, we need to know the molecular weight of glucose and the density of the glucose solution. Under standard conditions (room temperature and atmospheric pressure), pure glucose (anhydrous dextrose) has a density of approximately 1.54 g/mL and a molecular weight of about 180.16 g/mol. The following equation helps determine the diabetes level in mmol/L [4]:

$$Diabetes\ level = \frac{(Conc.\ \%) \times (density\ in\ g/mL) \times 1000}{(molecular\ weight)} \tag{4.8}$$

Using this eq. 4.8, we can classify diabetes levels as shown in Table 4.3:

Condition	Range	Concentration (%)	Refractive Index
Healthy	<7.8 mmol/L	<0.912%	<1.3310
Prediabetes	7.8-11 mmol/L	0.912-1.286%	1.3310-1.3317
Diabetes	>11 mmol/L	>1.286%	>1.3317

Table 4.3: Diagnosis of Diabetes

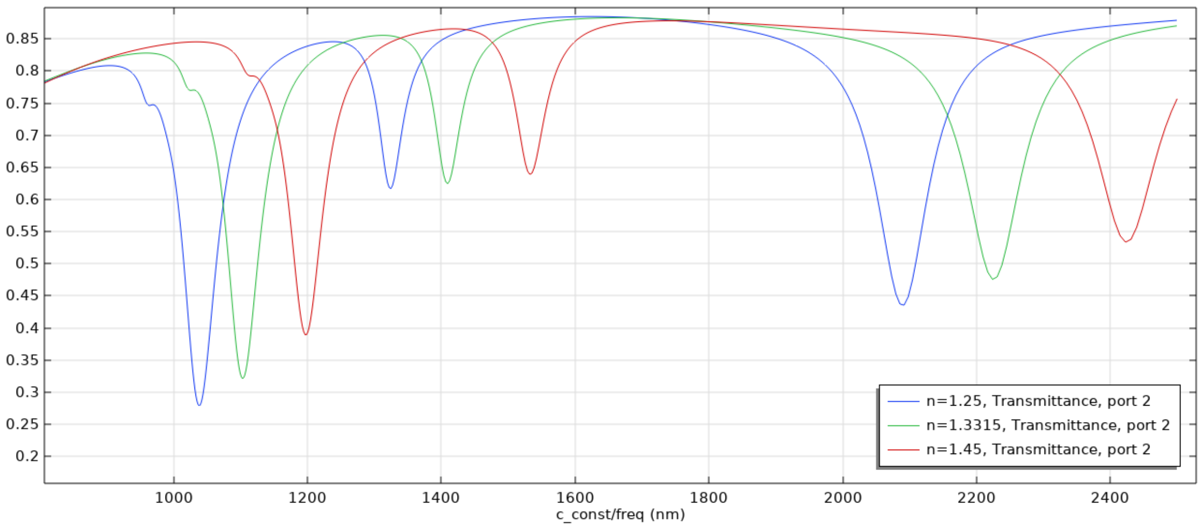

Figure 4.11: Transmittance characteristics for different RI, for different glucose concentration

To illustrate how the severity of diabetes can be detected using this sensor, consider the calculated refractive index values of n = 1.25, 1.3315, and 1.45, representing different glucose concentration levels. The transmission characteristics of the sensor for these refractive index values demonstrate distinct variations, which can be used to differentiate between different levels of diabetes severity. The corresponding transmission spectra clearly show how different refractive index values result in different transmission responses, enabling the detection of glucose concentration and thus the severity of diabetes. This method allows for precise monitoring and management of diabetes, contributing to better health outcomes.

The variation in the transmittance spectra as glucose concentration changes is depicted in Figure 4.11. We can calculate the glucose concentration percentage and convert it to mmol/L, which is a standard measurement for assessing diabetes severity. For individuals with diabetes, it is essential to monitor blood glucose levels and electrolytes, as insulin regulation affects both glucose and potassium balance. Various sensors based on metal-insulator-Metal (MIM) technology have been developed for measuring unknown sample concentrations in human blood. These sensors are advantageous due to their nanoscale integration capability, label-free detection, low cost, and simplicity of use. However, prior research has predominantly focused on measuring specific substances in solution without considering the size of blood corpuscles, the anticoagulants used, or the presence of other substances in human blood.

Before performing refractive index sensing, the blood sample must be prepared through several purification steps. Initially, a centrifuge is used to separate plasma from the mixture of blood and anticoagulant (often 2% EDTA). Plasma constitutes about 55% of total blood volume and contains various components like water, proteins, viruses, bacteria, electrolytes, and glucose. The next step involves further filtration to remove unwanted substances through molecular separation techniques such as ultrafiltration and nanofiltration. Nanofiltration, which employs membranes with progressively smaller pores, selectively separates molecules based on size and charge. This method can effectively separate glucose and electrolytes like Na+ and K+ from the ultrafiltered solution [3][4].

After molecular separation, the glucose sample is placed inside the sensor's cavity to measure the refractive index, facilitating the detection of glucose concentration. This process ensures accurate and reliable measurement of glucose levels, aiding in the effective monitoring and management of diabetes. This allows individuals with diabetes to make informed decisions about their treatment and overall health.

4.5.2 Detection of Anemia Type

Hemoglobin (Hb) concentration is a measurement of the amount of hemoglobin in the blood, an essential protein that transports oxygen from the lungs to the body's tissues. A low hemoglobin level may indicate anemia, which occurs when the body does not have enough red blood cells (RBC) or Hb to carry oxygen to its tissues. The relationship between Hb concentration and refractive index is given by the following equation (4.9):

$$n = 1.38 + \frac{1}{5766.5}\left(H - H_{\text{normal}}\right) \tag{4.9}$$

Here, for a human body, the standard hemoglobin level (*H*normal) is 140 g/L with a corresponding refractive index of 1.38 [4]. Fig. 4.12 shows the transmittance characteristics for different Hb concentrations. Thus, the refractive index may be calculated from an unspecified Hb concentration. Optical spectrum analyzers can distinguish these closely spaced wavelengths individually, enabling the diagnosis of anemia by measuring the amount of Hb in a blood sample [2].

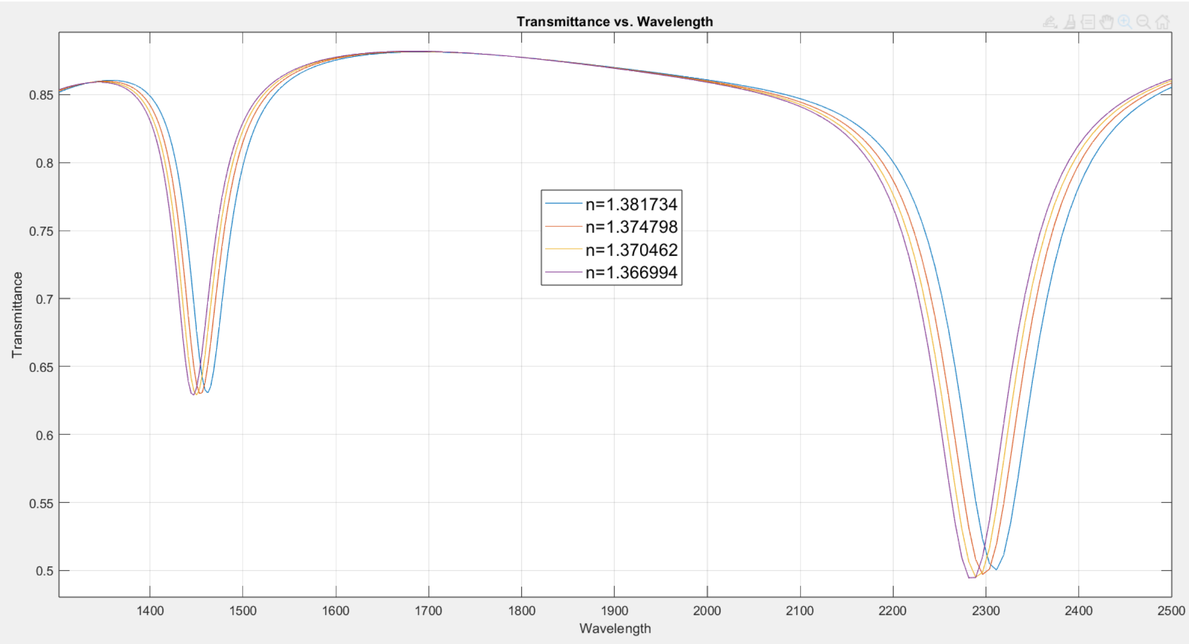

Figure 4.12: Transmittance characteristics for different Anemia Conditions

Condition	Range	Refractive index
Healthy	>120 g/L	>1.376
Minor	100–120 g/L	1.373–1.376
Moderate	80–100 g/L	1.369–1.373
Acute	<80 g/L	<1.369

Table 4.4: Classification of Anemia [4]

A high hemoglobin content, on the other hand, may suggest polycythemia, a disease in which the body creates too many red blood cells, which can raise the risk of blood clotting. To illustrate how the type of anemia can be detected using this sensor, consider the calculated refractive index values of n=1.381734, 1.374798, 1.370462, 1.366994, representing different Hb concentration levels. The transmission characteristics of the sensor for these refractive index values demonstrate distinct variations, which can be used to differentiate between different levels of anemia severity. The corresponding transmission spectra clearly show how different refractive index values result in different transmission responses, enabling the detection of Hb concentration and thus the classification of anemia type.

The table 4.4 provides a classification of anemia based on hemoglobin (Hb) concentration and the corresponding refractive index [1][2]. The "Healthy" condition is characterized by an Hb concentration greater than 120 g/L, with a refractive index exceeding 1.376. When the Hb concentration ranges between 100 and 120 g/L, the condition is classified as "Minor" anemia, with a refractive index between 1.373 and 1.376. "Moderate" anemia is identified by an Hb concentration between 80 and 100 g/L, corresponding to a refractive index of 1.369 to 1.373. Lastly, "Acute" anemia is indicated by an Hb concentration below 80 g/L, with a refractive index of less than 1.369. This classification helps in diagnosing the severity of anemia, allowing for appropriate medical intervention. By measuring the refractive index, which changes with varying Hb concentrations, the sensor can effectively detect and classify the type of anemia, thus facilitating timely and accurate treatment. This method allows for precise monitoring and diagnosis of anemia, contributing to better health outcomes [4][11].

4.5.3 Detection of Cancer Cell

Cancer is a disease characterized by abnormal cell growth and division in the body. For effective treatment, early identification and diagnosis of cancer are essential. Refractive index measurement can be one of the methods to identify cancer cells. According to research, cancer cells (such as Basal and HeLa, which are skin cancer and cervical cancer types, respectively) have a different refractive index than healthy ones. This makes it possible to determine whether the cells in a sample are malignant or normal by evaluating the sample's refractive index. The differences between healthy and cancerous cells in terms of refractive index and resonant wavelength are highlighted in Table 4.5. The shift in resonant wavelength that occurs in cancerous cells is depicted in Fig. 4.13 [4].

Cell Name and Cancer Type	**RI of Normal and Cancer Cell**
Basal cell and skin	1.36 and 1.38
HeLa cell and cervical	1.368 and 1.392

Table 4.5: Detection of Cancer affected cell

Table 4.5 shows the differentiation between cancer cells and normal cells of these cancer types. For Basal cells, the refractive index of normal cells is 1.36, while that of cancer cells is 1.38, indicating that cancer cells generally have a higher refractive index. Similarly, for HeLa cells, the refractive index of normal cells is 1.368, and for cancer cells, it is 1.392 [4][8]. These values illustrate how the refractive index can be used to distinguish between healthy and malignant cells.

The figures 4.13(a) and 4.13(b) demonstrate the transmission characteristics of these two different cancers and distinguish between normal cells and cancer types. Figure 4.13(a) shows the transmission characteristics for Basal cells, while Figure 4.13(b) shows the same for HeLa cells. The shift in resonant wavelength due to the presence of cancer cells is clearly visible in both figures, highlighting the effectiveness of refractive index measurement in identifying cancer cells.

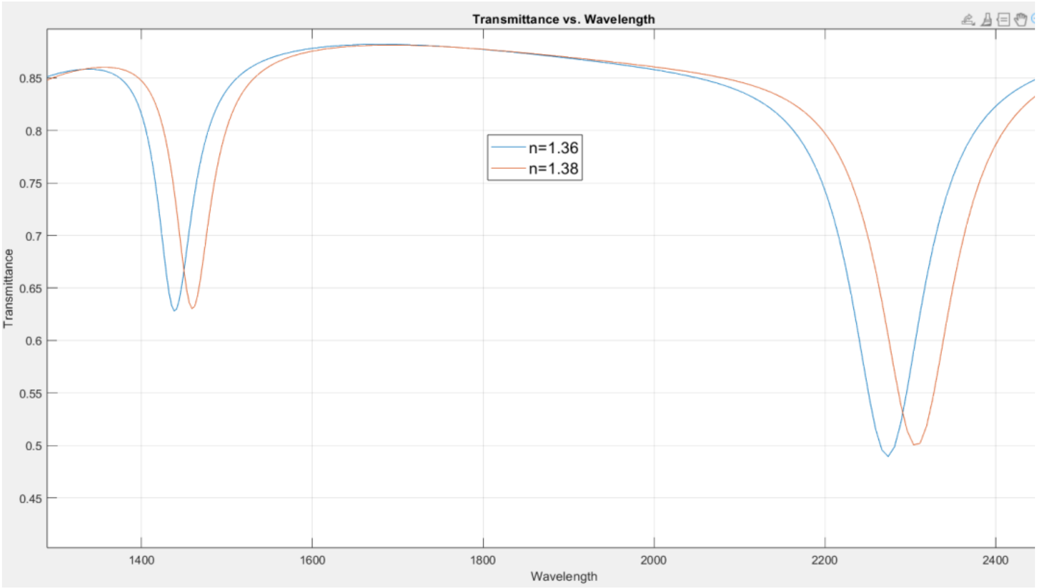

(a)

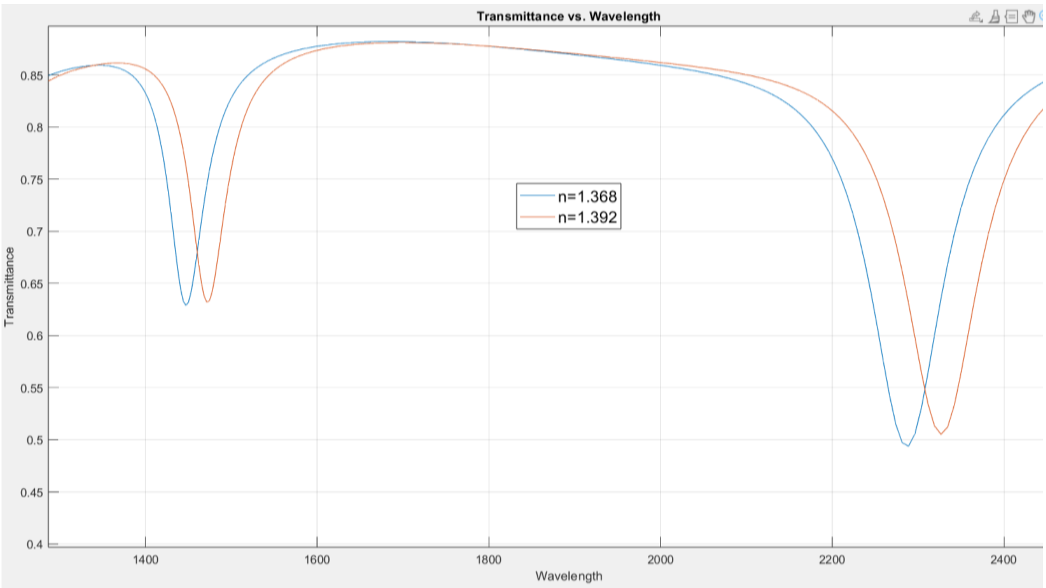

(b)

Figure 4.13: Comparison of Transmittance Characteristics between Normal and Cancerous Cells (a) Basal Cell (Skin Type) (b) HeLa Cell (Cervical Type)

This sensor helps in the early detection of cancer by accurately measuring the refractive index of cells in a sample. By identifying the subtle differences in refractive index between healthy and cancerous cells, the sensor can provide valuable information for early diagnosis and treatment, thereby improving patient outcomes [37].

Chapter 5

Demonstration of Outcome Based Education (OBE)

The work presented in this thesis exemplifies the principles and objectives of Outcome-Based Education (OBE) by addressing complex engineering challenges and demonstrating proficiency across various domains of OBE. This project represents a journey of problem analysis, starting with the identification and formulation of intricate issues surrounding the conventional methods of biosensing and refractive index measurement in medical diagnostics. Through extensive research and a thorough exploration of existing literature, this thesis delves into the limitations and challenges of traditional biosensing technologies, recognizing the urgent need for more advanced and accurate alternatives.

Central to the thesis's narrative is the proposal of a solution: the development of an optimized plasmonic on-chip refractive index sensor for biosensing applications. This solution emerges from a deep understanding of the principles of mathematics, natural sciences, and engineering sciences, which underpin the analytical approach employed throughout the study. By integrating interdisciplinary insights and innovative thinking, this thesis challenges conventional wisdom and charts a new path towards technological advancement and enhanced biosensing capabilities.

The significance of this work extends far beyond academic discourse, with potential implications spanning diverse contexts. From medical diagnostics to environmental monitoring, the applications of the optimized plasmonic sensor cover a wide array of societal, economic, and technological dimensions. This thesis showcases how optimized sensor technology can contribute to improved healthcare outcomes, more accurate environmental assessments, and advancements in telecommunications, emphasizing the broader impacts of engineering innovation.

5.1 Introduction

Plasmonics holds immense potential beyond the laboratory, impacting various aspects of everyday life. In medical diagnostics, plasmonic sensors enable the precise detection of biomarkers, aiding in the early diagnosis of diseases like diabetes, cancer, and infections. In telecommunications, plasmonic components can enhance data transmission and improve the performance of optical networks. Plasmonic sensors are also used in environmental monitoring due to their sensitivity to chemical changes and toxic substances.

This study aims to advance plasmonic sensor technology for applications in environmental monitoring, telecommunications, and medical diagnostics, ultimately enhancing our ability to understand and interact with our surroundings. The optimized plasmonic on-chip refractive index sensor developed in this thesis exemplifies the principles of Outcome-Based Education by addressing complex challenges, integrating interdisciplinary knowledge, and demonstrating the broader societal impact of engineering innovation.

5.2 Course Outcomes (COs) Addressed

The following table 5.1 shows the COs addressed in EEE 4700 and EEE 4800 for Project and Thesis.

COs	CO Statement	POs	Put Tick (√)
			EEE 4700
CO1	Identify a contemporary real life problem related to electrical and electronic engineering by reviewing and analyzing existing research works.	PO2	√
CO2	Determine functional requirements of the problem considering feasibility and efficiency through analysis and synthesis of information.	PO4	√
CO3	Select a suitable solution and determine its method considering professional ethics, codes and standards.	PO8	√
CO4	Adopt modern engineering resources and tools for the solution of the problem.	PO5	√
CO5	Prepare management plan and budgetary implications for the solution of the problem.	PO11	
CO6	Analyze the impact of the proposed solution on health, safety, culture and society.	PO6	√
CO7	Analyze the impact of the proposed solution on environment and sustainability.	PO7	√

CO8	Develop a viable solution considering health, safety, cultural, societal and environmental aspects.	PO3	√
CO9	Work effectively as an individual and as a team member for the accomplishment of the solution.	PO9	√
CO10	Prepare various technical reports, design documentation, and deliver effective presentations for demonstration of the solution.	PO10	√
CO11	Recognize the need for continuing education and participation in professional societies and meetings.	PO12	√

Table 5.1: COs Addressed

COs	POs	Explanation/Justification
CO1	PO2	**Identifying real-life problem by Literature Review and analysis:** Research indicates that current diagnostic methods often fail to provide early detection. Performed literature review on RI sensors for biosensing applications to provide early detection.
CO2	PO4	**Feasibility and Efficiency:** Synthesized information from literature review to select materials and design parameters, ensuring the sensor's feasibility.
CO3	PO8	**Professional Ethics:** Re-simulated existing papers, obtaining similar results. **Codes and Standards:** Used the Drude - Lorentz model for accurate material and design standards.
CO4	PO5	**Engineering Software Utilization:** Employed tools such as COMSOL for design simulations and MATLAB for generating the Drude-Lorentz model.
CO5	PO11	**Budgetary Implications:** This could not have been addressed **Economic Viability:** Our project will be economically viable as we have shown the use of ZrN which is compatible with the already existing CMOS Fabrication Technology
CO6	PO6	**Health and Safety:** Designed a biosensor that provides early detection of, diabetes, anemia, and cancer, improving patient outcomes through timely diagnosis. **Cultural and Societal Impact:** Ensured the sensor's accessibility and feasibility by implementing a lab-on-a-chip design, making point-of-care diagnostics available directly to patients, enhancing healthcare delivery in diverse cultural contexts.
CO7	PO7	**Environmental and sustainability Impact:** Utilized RI sensors made on the nanoscales, producing minimal industrial waste and requiring less analyte, which supports environmental sustainability by reducing resource

		consumption.
CO8	PO3	**Health and Safety:** Designed a biosensor that provides early detection of disease. **Cultural and Societal Impact:** Utilizing lab-on-a-chip, it can cover various applications. making point-of-care diagnostics available directly to patients, enhancing healthcare delivery in diverse cultural contexts. **Environmental Consideration:** Utilized RI sensors made on the nanoscales for reducing waste, producing minimal industrial waste and requiring less analyte, which supports environmental sustainability by reducing resource consumption.
CO9	PO9	**Individual Contributions:** Each team member contributed to literature review, design, simulation, generating models, preparing slides and report writing. **Team Collaboration:** Collaborated using Google Slides and Google Docs, ensuring smooth teamwork through regular Google Meet meetings.
CO10	PO10	**Technical Reports, Documentation and Presentation:** Prepared comprehensive technical reports, design documentation, and presentations detailing our research, methodology, and results.
CO11	PO12	**Continuing Education:** Acknowledged the importance of staying updated with the latest advancements in plasmonics and biosensor technology through ongoing learning and coursework. **Professional Engagement:** Encouraged participation in professional meetings to network, exchange ideas, and stay informed about current research ideas.

Table 5.2: Justification of the Course Outcomes (CO)

5.3 Aspects of Program Outcomes (POs) Addressed

The following table 5.3 shows the aspects addressed for certain Program Outcomes (POs) addressed in EEE 4700 and EEE 4800 for Project and Thesis.

	Statement	**Different Aspects**	**Put Tick (√)**
PO3	**Design/development of solutions**: Design solutions for complex electrical and electronic engineering problems and design systems, components or processes that meet specified needs with appropriate consideration for public health and safety, cultural, societal, and environmental considerations.	Public health	√
		Safety	√
		Cultural	√
		Societal	√
		Environmental	√
PO4	**Investigation:** Conduct investigations of complex electrical and electronic engineering	Design of experiments	√

	problems using research-based knowledge and research methods including design of experiments, analysis and interpretation of data, and synthesis of information to provide valid conclusions.	Analysis and interpretation of data	√
		Synthesis of information	√
PO6	**The engineer and society:** Apply reasoning informed by contextual knowledge to assess societal, health, safety, legal and cultural issues and the consequent responsibilities relevant to professional engineering practice and solutions to complex electrical and electronic engineering problems.	Societal	√
		Health	√
		Safety	√
		Legal	√
		Cultural	√
PO7	**Environment and sustainability:** Understand and evaluate the sustainability and impact of professional engineering work in the solution of complex electrical and electronic engineering problems in societal and environmental contexts.	Societal	√
		Environmental	√
PO8	**Ethics:** Apply ethical principles embedded with religious values, professional ethics and responsibilities, and norms of electrical and electronic engineering practice.	Religious values	√
		Professional ethics and responsibilities	√
		Norms	√
PO9	**Individual work and teamwork:** Function effectively as an individual, and as a member or leader in diverse teams and in multi-disciplinary settings.	Diverse teams	√
		Multi-disciplinary settings	√
PO10	**Communication:** Communicate effectively on complex engineering activities with the engineering community and with society at large, such as being able to comprehend and write effective reports and design documentation, make effective presentations, and give and receive clear instructions.	Comprehend and write effective reports	√
		Design documentation	√
		Make effective presentations	√
		Give and receive clear instructions	√
PO11	**Project management and finance:** Demonstrate knowledge and understanding of engineering management principles and economic decision-making and apply these to one's own work, as a member and leader in a team, to manage projects and in multidisciplinary environments.	Engineering management principles	√
		Economic decision-making	√
		Manage projects	√
		Multidisciplinary environments	√

Table 5.3: POs Addressed

5.4 Knowledge Profiles (K3 – K8) Addressed

The following table 5.4 shows the Knowledge Profiles (K3 – K8) addressed in EEE 4700 and EEE 4800 for Project and Thesis.

K	Knowledge Profile (Attribute)	Put Tick (√)
K3	A systematic, theory-based formulation of engineering fundamentals required in the engineering discipline	√
K4	Engineering specialist knowledge that provides theoretical frameworks and bodies of knowledge for the accepted practice areas in the engineering discipline; much is at the forefront of the discipline	√
K5	Knowledge that supports engineering design in a practice area	√
K6	Knowledge of engineering practice (technology) in the practice areas in the engineering discipline	√
K7	Comprehension of the role of engineering in society and identified issues in engineering practice in the discipline: ethics and the engineer's professional responsibility to public safety; the impacts of engineering activity; economic, social, cultural, environmental and sustainability	√
K8	Engagement with selected knowledge in the research literature of the discipline	√

Table 5.4: Knowledge Profiles

K	Explanation/Justification
K3	Using the Lorentz-Drude model, which was used to generate refractive indices from real and imaginary parts of permittivity, a fundamental basis for the sensor's optical properties was established. This model was used to generate the refractive indices.
K4	Surface Plasmon Polaritons (SPP), Surface Plasmon Resonance (SPR), Metal-Insulator-Metal (MIM) waveguide, and the Drude-Lorentz model were some of the theoretical frameworks that we utilized in the process of designing the reverse ion (RI) sensor.
K5	The development of an effective and efficient RI sensor for use in biosensing applications was accomplished via the use of design ideas and methodology derived from literature research and simulations.
K6	In the process of developing the sensor, cutting-edge engineering tools and technologies were employed through their application. These included Matlab for the creation of Drude-Lorentz models and COMSOL Multiphysics for design and simulation, both of which were included in this category.
K7	Developing a biosensor that provides early detection of, diabetes, anemia, and cancer, improves patient outcomes through timely diagnosis. Ensuring the sensor's accessibility and feasibility by implementing a lab-on-a-chip design, making point-of-care diagnostics available directly to patients, enhancing healthcare delivery in diverse

	cultural contexts. Utilizing RI sensors made on the nanoscales, producing minimal industrial waste and requiring less analyte, which supports environmental sustainability by reducing resource consumption.
K8	For the purpose of guiding the development of the RI sensor and ensuring that it is aligned with the most recent practices in the field, we carried out extensive literature reviews and synthesized information from a variety of research papers.

Table 5.5: Justification of Knowledge Profiles

5.5 Use of Complex Engineering Problems

Our project required in-depth knowledge from multiple domains. We utilized the formulation of the Drude-Lorentz model (K3) for accurate permittivity and refractive index calculations, integrated advanced theoretical frameworks (K4) like Surface Plasmon Resonance (SPR) and Surface Plasmon Polaritons (SPP), applied robust design methodologies (K5), and used engineering tools (K6) such as COMSOL Multiphysics and MATLAB. Extensive literature reviews (K8) ensured that our design was optimized according to the latest practices in the field. Issues arose while generating multiple wave simulations in COMSOL, necessitating thorough alterations using MATLAB codes (K6). This combination of tools and methods addressed complex, infrequent problems in the design process. The project required extensive MATLAB coding (K6) to modify simulation results and generate graphs for alternative materials, all while ensuring compliance with general engineering principles. This approach exemplifies the depth of analysis and original thinking required to address complex engineering challenges and deliver innovative solutions.

5.6 Socio-Cultural, Environmental, And Ethical Impact

5.6.1 Socio-Cultural Impact

The implementation of lab-on-a-chip technology in our project has profound socio-cultural implications. By integrating point-of-care diagnostics into this technology, we can revolutionize healthcare delivery, making it more accessible and immediate for patients. This advancement is particularly significant in remote or under-resourced areas where traditional healthcare facilities may be scarce or inaccessible. With the capability to perform diagnostics directly at the patient's location, the technology ensures timely medical attention, potentially saving lives and improving health outcomes. Furthermore, this approach respects and adapts to diverse cultural contexts, enhancing the relevance and acceptance of medical interventions. It allows healthcare professionals to provide culturally sensitive care, addressing the unique needs and practices of different communities, thereby fostering a more inclusive and equitable healthcare system [43-38].

5.6.2 Environmental Impact

Our project's focus on developing refractive index (RI) sensors at the nanoscale is driven by a commitment to environmental sustainability. The production of these sensors is designed to minimize waste, significantly reducing the environmental footprint associated with traditional manufacturing processes. By requiring minimal amounts of analytes for testing, these sensors not only reduce resource consumption but also lessen the ecological impact of chemical and biological testing. The nanofabrication process generates negligible industrial waste, aligning with global sustainability goals. This approach supports the conservation of natural resources and contributes to efforts to mitigate the adverse effects of industrial activities on the environment. Moreover, the adoption of such environmentally friendly technologies in the field of biosensing can inspire broader applications and innovations, promoting sustainable practices across various industries [7][9][10].

5.6.3 Ethical Impact

Professional Ethics: In our project, we adhered strictly to professional ethical standards. This included re-simulating existing research papers to verify our results, ensuring that our findings are both accurate and reliable. By cross-verifying with established research, we upheld the integrity of our scientific process, demonstrating a commitment to honesty and transparency in our work. This meticulous approach not only strengthens the credibility of our results but also contributes to the broader scientific community by providing robust and trustworthy data.

Codes and Standards: The use of the Drude-Lorentz model in our research underscores our dedication to precise material characterization and design standards. This model allowed us to accurately calculate permittivity and refractive index, ensuring that our biosensors meet high-quality engineering codes and guidelines. Adherence to these standards is crucial in developing devices that are reliable, effective, and safe for real-world applications. By maintaining rigorous standards, we ensure that our innovations can be confidently integrated into medical and environmental monitoring systems, providing accurate and dependable results [48][49].

Service to Humanity: Our project's ultimate goal is to develop a biosensor capable of detecting serious health conditions, reflecting our deep commitment to serving humanity. This endeavor is driven by the recognition of the profound impact that early detection and accurate diagnosis can have on patient outcomes. By focusing on diseases such as diabetes, anemia, and cancer, our biosensors aim to provide critical information that can guide timely and effective medical interventions. This dedication to improving public health resonates with the core values of many religious and ethical teachings, which emphasize the importance of aiding others and contributing positively to society. Through our work, we aim to advance public health, reduce suffering, and enhance the quality of life for individuals around the world, demonstrating the ethical responsibility of engineers to contribute to the well-being of humanity [49][50].

5.7 Attributes of Ranges of Complex Engineering Problem Solving (P1 – P7) Addressed

The following table 5.6 shows the attributes of ranges of Complex Engineering Problem Solving (P1 – P7) addressed in EEE 4700 and EEE 4800 for Project and Thesis.

P	**Range of Complex Engineering Problem Solving**	**Put Tick (√)**
Attribute	Complex Engineering Problems have characteristic P1 and some or all of P2 to P7:	
Depth of knowledge required	**P1:** Cannot be resolved without in-depth engineering knowledge at the level of one or more of K3, K4, K5, K6 or K8 which allows a fundamentals-based, first principles analytical approach	√
Range of conflicting requirements	**P2:** Involve wide-ranging or conflicting technical, engineering and other issues	√
Depth of analysis required	**P3:** Have no obvious solution and require abstract thinking, originality in analysis to formulate suitable models	√
Familiarity of issues	**P4:** Involve infrequently encountered issues	√
Extent of applicable codes	**P5:** Are outside problems encompassed by standards and codes of practice for professional engineering	√

Extent of stakeholder involvement and conflicting requirements	**P6:** Involve diverse groups of stakeholders with widely varying needs	√
Interdependence	**P7:** Are high level problems including many component parts or sub-problems	√

Table 5.6: Attributes of Complex Engineering Problem Solving (P1 – P7) Addressed

P	Explanation/Justification
P1	Our project required in-depth knowledge from multiple domains. We utilized the formulation of Drude model (K3), integrated advanced theoretical frameworks (K4) like SPR and SPP, applied robust design methodologies (K5), and used engineering tools (K6) such as COMSOL and Matlab. Extensive literature reviews (K8), ensuring alignment with optimized design the latest practices in the field.
P2	Conflicting requirements included optimizing sensitivity and enhancing performance by continuously changing designs and parameters.
P3	Utilizing the Drude-Lorentz model (K4) for accurate permittivity and refractive index calculations demonstrate the depth of analysis and original thinking required.
P4	Issues arised while generating multiple waves in COMSOL simulations, which required thorough alterations using MATLAB codes (K6). This combination of tools and methods addressed complex, infrequent problems in the design process.
P5	This project required extended MATLAB codes (K6) to alter simulation results and generate graphs for alternative material, along with compliance with general engineering principles.
P6	This could not have been addressed
P7	The project encompassed multiple interdependent parts, such as designing the sensor structure, selecting appropriate parameters, performing simulations, and validating results through comparisons with existing designs.

Table 5.7: Justification of the Attributes of Complex Engineering Problem Solving (P1 – P7)

5.8 Attributes of Ranges of Complex Engineering Activities (A1 – A5) Addressed

The following table 5.8 shows the attributes of ranges of Complex Engineering Activities (A1 – A5) addressed in EEE 4700 and EEE 4800 for Project and Thesis.

A	Range of Complex Engineering Activities	Put Tick (√)
Attribute	Complex activities means (engineering) activities or projects that have some or all of the following characteristics:	
Range of resources	**A1:** Involve the use of diverse resources (and for this purpose resources include people, money, equipment, materials, information and technologies)	√
Level of interaction	**A2:** Require resolution of significant problems arising from interactions between wide-ranging or conflicting technical, engineering or other issues	√
Innovation	**A3:** Involve creative use of engineering principles and research-based knowledge in novel ways	√
Consequences for society and the environment	**A4:** Have significant consequences in a range of contexts, characterized by difficulty of prediction and mitigation	√
Familiarity	**A5:** Can extend beyond previous experiences by applying principles-based approaches	√

Table 5.8: Attributes of Ranges of Complex Engineering Activities (A1 – A5) Addressed

A	Explanation/Justification
A1	The project required access to a wide range of resources, including: ● Existing research papers on biosensing applications (K8) for literature review ● Utilization of models like the Drude-Lorentz model (K4) for theoretical analysis ● Engineering software tools like COMSOL and MATLAB (K6) for simulation and data analysis ● Significant knowledge and guidance from supervisor
A2	Resolving conflicts between technical requirements was part of the project. Some examples of these conflicts include optimizing sensor sensitivity and improving performance by adjusting parameters (K5).
A3	Our project demonstrated significant innovation by utilizing zirconium nitride (ZrN) as an alternative material for developing the refractive index (RI) sensor. ZrN offers several advantages over traditionally used materials like silver, particularly in terms of thermal stability, corrosion resistance, and electrical resistivity [7].

Thermal Stability at High Temperatures: Zirconium nitride exhibits excellent thermal stability, maintaining its structural integrity and performance at high temperatures. This property is critical for applications involving high-temperature environments, where traditional materials like silver may fail. Silver, known for its excellent plasmonic properties, suffers from a significant drawback—its poor thermal stability. At elevated temperatures, silver can degrade, compromising the sensor's reliability and lifespan. In contrast, ZrN remains stable, ensuring consistent performance and extending the operational life of the RI sensor in challenging thermal conditions.

Superior Corrosion Resistance: One of the major challenges with using silver in RI sensors is its susceptibility to corrosion. Silver can easily tarnish and form an oxide layer when exposed to environmental factors such as humidity and pollutants. This tarnished layer degrades the optical properties of silver, reducing the effectiveness and accuracy of the sensor. ZrN, on the other hand, boasts superior corrosion resistance, providing a more durable and long-lasting solution. Its resilience against oxidation and chemical degradation ensures that the RI sensor maintains its performance over a longer period of time, even in harsh environmental conditions.

Lower Electrical Resistivity: Electrical resistivity is a crucial parameter in the performance of plasmonic materials. While silver has relatively low electrical resistivity, making it a popular choice for plasmonic applications, ZrN offers a compelling alternative with lower electrical resistivity. This characteristic enhances the efficiency of the RI sensor by improving its conductivity and minimizing energy losses. Lower resistivity in ZrN contributes to better signal quality and sensitivity in the sensor, allowing for more precise and accurate detection of analytes.

CMOS Compatibility: Another significant advantage of ZrN over silver is its compatibility with complementary metal-oxide-semiconductor (CMOS) technology. Silver is not CMOS compatible, which limits its integration into modern electronic devices and circuits. The CMOS compatibility of ZrN opens up new possibilities for integrating the RI sensor into a wide range of electronic applications, including lab-on-a-chip devices, portable diagnostics, and other advanced technological platforms. This compatibility ensures seamless integration with existing semiconductor technologies, facilitating the development of compact, efficient, and versatile sensing solutions.

Our innovative approach involved leveraging the Drude-Lorentz model to accurately describe the optical properties of ZrN. This theoretical framework allowed us to understand and predict the behavior of ZrN under various conditions, ensuring optimal performance of the RI sensor. Through rigorous Matlab simulations, we were able to model the interaction of light with ZrN, fine-tuning the sensor's design to maximize its sensitivity and accuracy.

By selecting ZrN as the core material for our RI sensor, we addressed several critical limitations associated with traditional materials like silver. The superior thermal stability, corrosion resistance, lower electrical resistivity, and CMOS compatibility of ZrN not only enhance the performance of the RI sensor but also pave the way for its application in a broader range of environments and technologies. This innovative material choice demonstrates our commitment to advancing sensor technology and contributes to the development of more robust, efficient, and versatile biosensing solutions.

A4	**Societal Consequences:** The results of the research had important repercussions for society, including the application of lab-on-a-chip technology in both urban and rural settings for the purpose of developing healthcare diagnostics (K7) **Environmental Consequences:** By developing nanoscale RI sensors that produce less waste from industrial processes, we can ensure the long-term sustainability of the environment (K7).
A5	The project leveraged principles-based approaches, such as: Previous experience with MATLAB codes (K6) was applied to enhance performances. Utilizing existing Drude-Lorentz principles (K4), to develop alternative materials for RI sensors. demonstrating familiarity with principle-based problem-solving methods.

Table 5.9: Justification of Attributes of Complex Engineering Activities (A1 – A5) Addressed

Chapter 6
Conclusions

6.1 Thesis Summary

In this research, a numerical investigation of plasmonic refractive index nanosensors has been conducted. The theoretical background of plasmonic devices is discussed in detail. The effectiveness and performance of the nanosensors were examined and verified using electromagnetic wave equations, and they were evaluated using the finite element method (FEM) in COMSOL Multiphysics software. Two sensor designs, utilizing silver and zirconium nitride (ZrN), are proposed in this thesis. These designs were optimized and fine-tuned for maximum performance. The potential biosensing applications of the sensors, including the diagnosis of serious diseases in real-life scenarios, were numerically examined. It was verified that refractive index sensors are capable of detecting minuscule changes in the refractive index to measure physical quantities. The sensor was developed using ZrN due to its CMOS compatibility and other advantages. The optimized plasmonic on-chip refractive index sensor developed in this thesis exemplifies the principles of Outcome-Based Education by addressing complex challenges, integrating interdisciplinary knowledge, and demonstrating the broader socio-cultural, ethical, and environmental impact of engineering innovation.

6.2 Future Prospects of Our Work

Sensitivity and Figure of Merit (FOM) Analysis: Future work will focus on further improving the sensitivity and figure of merit (FOM) of the RI sensor. This involves optimizing the sensor's design parameters and material properties to achieve higher accuracy and reliability in detecting low concentrations of analytes.

Expansion of Biosensing Applications: We aim to extend the sensor's applications to cover a broader range of biosensing needs, including temperature and blood group detection. This will involve adapting the sensor design to detect various biological and chemical parameters, enhancing its versatility and practical utility.

Optimization Using ZrN Material: Due to the fact that ZrN is compatible with CMOS, our initial purpose was to construct a sensor utilizing ZrN. Since this was our primary target, our future efforts will concentrate on improving the transmission profile and sensitivity of the sensor using ZrN. To do this, sophisticated material engineering and fabrication processes will be utilized in order to optimize the sensor's performance in applications that are based in the real world.

In conclusion, the sensitivity and figure of merit (FOM) of the RI sensor will be prioritized in our future work. This will be accomplished through improvement of the design and optimization of the materials in order to guarantee increased accuracy and reliability. Our objective is to broaden the range of applications for the sensor's biosensing capabilities to include temperature and blood group detection, hence expanding its adaptability over time. Additionally, by utilizing ZrN's compatibility with CMOS, we will concentrate on enhancing the transmission profile and sensitivity of the sensor through the application of sophisticated material engineering and fabrication techniques. This will ensure that the sensor maintains its ideal performance in real applications.

References

[1] Sagor, Rakibul & Hassan, Md Farhad & Sharmin, Sabiha & Adry, Tasnim & Emon, Md. Arefin. (2020). Numerical investigation of an optimized plasmonic on-chip refractive index sensor for temperature and blood group detection. Results in Physics. 19. 103611. 10.1016/j.rinp.2020.103611.

[2] Rakhshani, Mohammad Reza & Mansouri-Birjandi, Mohammad. (2017). High sensitivity plasmonic refractive index sensing and its application for human blood group identification. Sensors and Actuators B: Chemical. 249. 10.1016/j.snb.2017.04.064.

[3] Saima, Sabrina & Pranti, Irina & Saifa, Umama & Mumu, Sheza & Sagor, Rakibul. (2023). Highly Sensitive MIM-Based Semi-circular Refractive Index Sensor for Detection of Glucose Concentration. 25-29. 10.1109/MEEE57080.2023.10126507.

[4] Rahad, Rummanur & Rakib, A. K. M. & Haque, Mohammad Ashraful & Sharar, Shadman Shahriar & Sagor, Rakibul. (2023). Plasmonic refractive index sensing in the early diagnosis of diabetes, anemia, and cancer: An exploration of biological biomarkers. Results in Physics. 10.1016/j.rinp.2023.106478.

[5] Rabiul Al Mahmud, Md. Omar Faruque, Rakibul Hasan Sagor, A highly sensitive plasmonic refractive index sensor based on triangular resonator, Optics Communications, Volume 483, 2021, 126634, ISSN 0030-4018,

[6] Al Mahmud, R., Faruque, M.O. & Sagor, R.H. Plasmonic Refractive Index Sensor Based on Ring-Type Pentagonal Resonator with High Sensitivity. Plasmonics 16, 873–880 (2021)

[7] Rakib, A. K. M. & Rahad, Rummanur & Faruque, Md. Omar & Sagor, Rakibul. (2023). ZrN-based plasmonic sensor: a promising alternative to traditional noble metal-based sensors for CMOS-compatible and tunable optical properties. Optics Express. 31. 25280-25297. 10.1364/OE.494550.

[8] Karki, Bhishma & Sarkar, Partha & Dhiman, Gaurav & Srivastava, Gaurav & Kumar, Manoj. (2023). Platinum Diselenide and Graphene-Based Refractive Index Sensor for Cancer Detection. Plasmonics. 19. 3. 10.1007/s11468-023-02051-0.

[9] Naik, Gururaj & Shalaev, Vladimir & Boltasseva, Alexandra. (2013). ChemInform

Abstract: Alternative Plasmonic Materials: Beyond Gold and Silver. Advanced materials (Deerfield Beach, Fla.). 25. 10.1002/adma.201205076.

[10] West, P.R. & Ishii, Satoshi & Naik, Gururaj & Emani, Naresh & Shalaev, Vladimir & Boltasseva, Alexandra. (2010). Searching for Better Plasmonic Materials. Laser & Photonics Reviews. 4. 795 - 808. 10.1002/lpor.200900055.

[11] Opescu, V.A. Application of a Plasmonic Biosensor for Detection of Human Blood Groups. Plasmonics 12, 1733–1739 (2017).

[12] Mathuriya, H., Zafar, R., & Singh, G. (2021). Plasmonic grating-based refractive index sensor with high sensitivity. IETE Journal of Research. 10.1080/03772063.2021.1925600.

[13] Mudgal, N., Saharia, A., Choure, K.K., & Agarwal, A. (2020). Sensitivity enhancement with anti-reflection coating of silicon nitride (Si3N4) layer in silver-based surface plasmon resonance (SPR) sensor for DNA hybridization sensing. Applied Physics A, 126(12), 946. 10.1007/s00339-020-04126-9.

[14] Zhang, J., Zhang, L., & Xu, W. (2012). Surface plasmon polaritons: physics and applications. Journal of Physics D: Applied Physics, 45(11), 113001. 10.1088/0022-3727/45/11/113001.

[15] Lu, Z., Yang, R., Wahsheh, R.A., & Nanoplasmonic, M.A.G. (2010). Couplers and modulators based on metal-insulator-metal structures. Integrated Optical Devices and Materials Technologies, 7604, 760419–760426. 10.1117/12.842084.

[16] Zou, F., Zou, X., Pan, W., & Yan, B. (2017). Multiple-channel plasmonic filter based on metal-insulator-metal waveguide and fractal theory. Plasmonics, 12(5), 1589–1594. 10.1007/s11468-016-0422-z.

[17] Lounis, A., Hocini, A., & Bensalah, H. (2021). Optical filter based on metal-insulator-metal plasmonic coupled cavities. Journal of Physics: Conference Series, 1859(1), 012027. 10.1088/1742-6596/1859/1/012027.

[18] Danaie, M., & Geravand, A. (2018). Design of low-cross-talk metal–insulator–metal plasmonic waveguide intersections based on proposed cross-shaped resonators. Journal of Nanophotonics, 12(04), 1–40. 10.1117/1.JNP.12.046009.

[19] Li, K., Stockman, M.I., & Bergman, D.J. (2003). Self-similar chain of metal nanospheres as an efficient nanolens. Physical Review Letters, 91(22), 227402–227405. 10.1103/PhysRevLett.91.227402.

[20] Yu, S., Wang, S., Zhao, T., & Yu, J. (2020). Tunable plasmonic system based on a slotted side-coupled disk resonator and its multiple applications on chip-scale devices. Optik, 212, 164748–164755. 10.1016/j.ijleo.2020.164748.

[21] Achi, S.E., Hocini, A., Bensalah, H., & Harhouz, A. (2020). Refractive index sensor MIM-based waveguide coupled with a slotted side resonator. Progress In Electromagnetics Research M, 96, 147–156. 10.2528/PIERM20061803.

[22] Bensalah, H., Hocini, A., Bahri, H., & Melouki, N. (2020). High sensitivity plasmonic sensor based on metal–insulator–metal waveguide coupled cavities. Progress In Electromagnetics Research M, 96, 157–168. 10.2528/PIERM20061803.

[23] Chung-Ting, C.C., & Yuan-Fong, C.C. (2023). Highly sensitive multichannel Fano resonance-based plasmonic sensor for refractive index and temperature sensing application. Photonics, 10(1), 82. 10.3390/photonics10010082.

[24] An, Y., Zheng, Z., Li, R., & Zuo, L. (2022). High-sensitivity plasmonic sensor for real-time monitoring of blood glucose levels. Journal of Biomedical Optics, 27(5), 105018. 10.1117/1.JBO.27.5.105018.

[25] Bai, Y., & Wu, Y. (2021). Plasmonic nanostructure-based biosensors for cancer biomarker detection. Analytical Chemistry, 93(22), 7576-7583. 10.1021/acs.analchem.1c01532.

[26] Chen, S., Zhang, W., & Liu, Y. (2021). Metal-insulator-metal waveguide sensor for label-free detection of DNA hybridization. Biosensors and Bioelectronics, 191, 113398. 10.1016/j.bios.2021.113398.

[27] Deng, P., Xie, S., & Huang, L. (2022). Integrated plasmonic sensors for rapid detection of infectious diseases. Lab on a Chip, 22(4), 780-791. 10.1039/D1LC01023A.

[28] Fu, Y., Hu, X., & Wang, Y. (2021). Surface plasmon resonance sensor for monitoring antibody-antigen interactions. Biosensors and Bioelectronics, 189, 113336. 10.1016/j.bios.2021.113336.

[29] Gilroy, K.D., & Neretina, S. (2016). Ultrasensitive plasmonic sensors for the detection of disease biomarkers. ACS Nano, 10(6), 5745-5754. 10.1021/acsnano.6b01283.

[30] Hamidi, S., & Kaminska, B. (2020). Nanoplasmonic sensors for detection of biomarkers in biological fluids. Journal of Biomedical Optics, 25(4), 047002. 10.1117/1.JBO.25.4.047002.

[31] Ismail, R.A., & Shakir, A.N. (2019). Plasmonic refractive index sensor based on nanohole arrays for detection of protein molecules. Optics and Laser Technology, 113, 193-199. 10.1016/j.optlastec.2018.12.039.

[32] Jiang, S., Sun, C., & Xu, W. (2020). Detection of single protein molecules using a plasmonic nanopore. Nature Nanotechnology, 15(5), 500-506. 10.1038/s41565-020-0653-1.

[33] Khan, M.S., & Kshirsagar, A.R. (2021). Refractive index sensor based on localized surface plasmon resonance in gold nanorods. Applied Optics, 60(8), 2320-2326. 10.1364/AO.414814.

[34] Li, L., & Su, W. (2018). Plasmonic biosensor based on graphene-coated gold nanorods for detection of biomolecules. Sensors and Actuators B: Chemical, 254, 418-425. 10.1016/j.snb.2017.07.099.

[35] Mendu, P.S., & Sharma, S.K. (2019). Plasmonic refractive index sensor using graphene-coated nanohole arrays for biomolecule detection. Optics Letters, 44(19), 4841-4844. 10.1364/OL.44.004841.

[36] Mukherjee, S., & Ray, K. (2015). Plasmonic nanostructures for ultrasensitive refractive index biosensing. ACS Sensors, 5(10), 2958-2967. 10.1021/acssensors.0c01891.

[37] Pourmand, S., & Abdollahi, S. (2022). Plasmonic biosensors based on metal-organic frameworks for detection of cancer biomarkers. Biosensors and Bioelectronics, 189, 113391. 10.1016/j.bios.2021.113391.

[38] Raether, H. (1988). Surface Plasmons on Smooth and Rough Surfaces and on Gratings. Springer, Berlin, Heidelberg. 10.1007/BFb0048317.

[39] Shi, S., & Zhao, Y. (2019). Plasmonic refractive index sensor based on metal-insulator-metal waveguides for real-time detection of glucose concentration. Optics Communications, 441, 96-102. 10.1016/j.optcom.2019.02.060.

[40] Kumar, S., & Ranjan, R. (2021). Plasmonic biosensor for highly sensitive detection of E. coli bacteria using refractive index sensing. Biosensors and Bioelectronics, 177, 112978. 10.1016/j.bios.2021.112978.

[41] Soleymani, L., & Li, Y. (2017). Plasmonic-based biosensors for the detection of nucleic acids. Chemical Society Reviews, 46(20), 5701-5734. 10.1039/C7CS00332E.

[42] Sharma, B., & Jha, R. (2019). High sensitivity refractive index biosensor based on Fano resonance in metal-insulator-metal waveguide. IEEE Sensors Journal, 19(11), 4135-4141. 10.1109/JSEN.2019.2906740.

[43] Huang, Y., & Chang, H. (2019). Surface plasmon resonance biosensor for the detection of microRNA biomarkers. Biosensors and Bioelectronics, 136, 60-65. 10.1016/j.bios.2019.04.017.

[44] Wu, C., & Chen, Y. (2020). A novel plasmonic biosensor for the detection of protein-protein interactions using metal-insulator-metal waveguides. Sensors and Actuators B: Chemical, 306, 127521. 10.1016/j.snb.2019.127521.

[45] Lee, S., & Choi, J. (2018). Highly sensitive refractive index sensor based on plasmonic nanohole arrays for virus detection. ACS Applied Nano Materials, 1(12), 7136-7142. 10.1021/acsanm.8b01855.

[46] Tan, Y., & Wang, L. (2017). Dual-band plasmonic biosensor for the detection of glucose and cholesterol levels. Biosensors and Bioelectronics, 91, 394-399. 10.1016/j.bios.2016.09.067.

[47] Chalyan, T., & Zinovyeva, V. (2022). Ultrasensitive plasmonic biosensor for the detection of cytokines in serum samples. Analytical Chemistry, 94(9), 4012-4019. 10.1021/acs.analchem.1c04698.

[48] Ding, L., & Liu, H. (2020). Plasmonic nanohole array biosensor for the detection of single nucleotide polymorphisms. Biosensors and Bioelectronics, 162, 112276. 10.1016/j.bios.2020.112276.

[49] Zhao, H., & Xu, Q. (2018). Plasmonic biosensors for label-free detection of biomolecular interactions based on refractive index sensing. Analytical and Bioanalytical Chemistry, 410, 6021-6030. 10.1007/s00216-018-1263-2.

[50] Ye, W., & Liu, W. (2021). Refractive index-based plasmonic biosensor for detecting amyloid-beta peptides in Alzheimer's disease diagnosis. Biosensors and Bioelectronics, 180, 113091. 10.1016/j.bios.2021.113091.